Electronic Supplementary Material (ESI) for ChemComm.

Thermo-responsive self-immolative nanoassemblies: Direct and indirect triggering

Bo Fan[1], John F. Trant[2], Gauvin Hemery[3], Olivier Sandre[3], Elizabeth R. Gillies*[1,2]

[1]Department of Chemical and Biochemical Engineering, The University of Western Ontario, 1151 Richmond St., London, Canada, N6A 5B9; E-mail: egillie@uwo.ca.
[2]Department of Chemistry, The University of Western Ontario, 1151 Richmond Street, London, Canada, N6A 5B7.
[3]Laboratoire de Chimie des Polymères Organiques (LCPO), Université de Bordeaux, Bordeaux INP, ENSCBP, 16 avenue Pey Berland, Pessac Cedex, France, 33607.

Table of Contents

1. Chemical structures of control polymers

a)

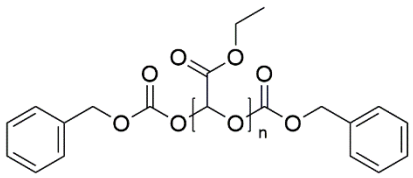

PEtG-control

b)

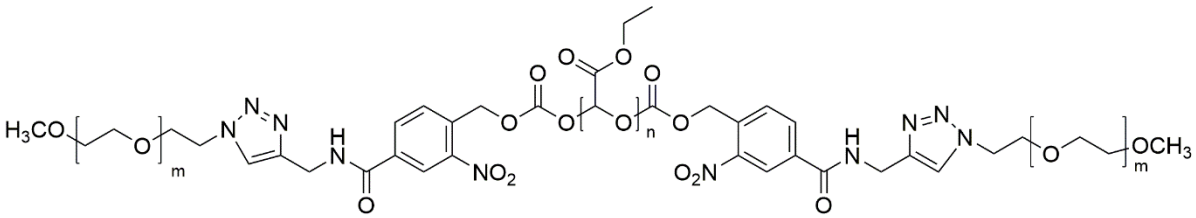

Micelle-control, m = 45

c)

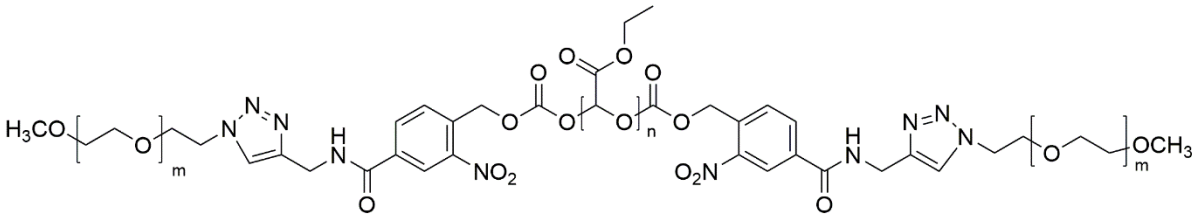

Vesicle-control, m = 17

Scheme S1. Chemical structure of a) **PEtG-control**, b) **Micelle-control**, and c) **Vesicle control**.

2. Experimental procedures

General materials and procedures. Micelle-control[1a] and **PEtG-control**[1b] were previously reported and the same batches were used here. Ethyl glyoxylate in toluene solution (50% w/w), 2-(hydroxymethyl)furan, diisopropylethylamine were obtained from Alfa Aesar (Canada). Nile red and phosgene solution (15 wt. % in toluene) were purchased from Sigma-Aldrich (USA). Iron dichloride tetra-hydrate powder ($FeCl_2.4H_2O$), iron trichloride hexahydrate 45% solution ($FeCl_3.6H_2O$), diethylene glycol, N-methyldiethanolamine, nitric acid were obtained from Sigma-Aldrich (France). Beycostat NE (Ref NB09) was obtained from CECA chemicals (France). Triethylamine, pyridine, and dichloromethane were distilled from calcium hydride before use. Anhydrous tetrahydrofuran, acetonitrile were obtained from a solvent purification

system using aluminum oxide columns. All the other chemicals were of reagent grade and used without further purification. ^{1}H NMR spectra were obtained at 400 MHz or 600 MHz on Varian Inova instruments. NMR chemical shifts (δ) are reported in ppm and were calibrated against residual solvent signals of $CDCl_3$ (δ 7.27), CD_3CN (δ 1.94), or D_2O (δ 4.75). Fourier transform infrared (FTIR) spectra were obtained in attenuated total reflectance (ATR) mode using a PerkinElmer UATR Spectrum Two with films drop cast from CH_2Cl_2 on diamond. High-resolution mass spectrometry (HRMS) was performed with either a Thermo Scientific DFS (Double Focus Sector) mass spectrometer, using a reversed Nier Johnson geometry for electron impact (EI) ionization, or a Bruker microOTOF 11 for electrospray ionization (ESI). The SEC instrument was equipped with a Viscotek GPC Max VE2001 solvent module. Samples were analyzed using the Viscotek VE3580 RI detector operating at 30 ˚C. The separation technique employed two Agilent Polypore (300 × 7.5mm) columns connected in series and to a Polypore guard column (50 × 7.5mm). Samples were dissolved in THF (glass distilled grade) at approximately 5 mg/mL and filtered through 0.22 μm syringe filters. Samples were injected using a 100 μL loop. The THF eluent was filtered and eluted at 1 mL/min for a total of 30 min. A calibration curve was obtained from poly(methyl methacrylate) standards with molecular weight ranges of 1,540-1,126,000/mol. Thermogravimetric analyses (TGA) were performed on a TGA Q50 from TA Instruments. The heating rate was 10 ˚C /min between 30-500 ˚C under N_2. Ultrapure water was obtained from a Barnstead EASYpure II system. Dialyses were performed using Spectra/Por regenerated cellulose membranes with 3500 g/mol molecular weight cut-off. The hydrodynamic diameters of the polymer assemblies were measured by dynamic light scattering (DLS) using a Zetasizer Nano Series ZS instrument from Malvern Instruments, at room temperature (25 ºC) in a 1 cm path length glass cuvette at a concentration of 0.8 mg/ml suspension of polymer assemblies. Fluorescence spectra were obtained using a QM-4 SE spectrometer from Photon Technology International (PTI) equipped with double excitation and emission monochromators. TEM imaging was performed using a Phillips CM10 microscope operating at an acceleration voltage of 80 kV. 3 μL of micelle suspension (0.08 mg / mL) was

placed onto a copper grid. The resulting sample was air-dried overnight before imaging. TEM for IONPs and IONPs loaded micelles was performed on a Hitachi H7650 microscope operated at 80 kV on samples deposited at ~1 mg/mL onto copper grids by a lab-made spraying tool.

Synthesis of Compound 3a. *N*-benzyl maleimide[2] (2.00 g, 10.7 mmol) and 2-(hydroxymethyl) furan (931 µL, 1.05 g, 10.7 mmol) were dissolved in anhydrous acetonitrile under a nitrogen atmosphere in a flame-dried flask equipped with a magnetic stirring-bar. The reaction was stirred at 35 ºC for 14 h. When TLC indicated the reaction had reached equilibrium, the solvent was removed, and the reaction was concentrated under reduced pressure for 1 h. NMR spectroscopy of the unpurified reaction product indicated a ratio of (1:0.4:0.3) of endo-exo-unreacted maleimide. The crude material was then purified by flash chromatography (6:4 to 4:6 hexanes-ethyl acetate) to provide 2.3 g of a mixture of the endo and exo in a 70:30 ratio and a 75 % isolated yield. A small amount of material was purified further by preparative TLC (8:2 hexanes-ethyl acetate, 7 elutions) to provide analytical samples of both the endo and exo products. Due to the inherent thermal instability, the material is stored at -20 ºC until needed. **3a-endo** ^{1}H NMR (600 MHz, $CDCl_3$): δ_{ppm} 7.31-7.26 (m, 5H), 6.15 (dd, *J* = 5.8, 1.5 Hz, 1H), 6.06 (d, *J* = 5.8 Hz, 1H), 5.26 (dd, *J* = 5.5, 1.6 Hz, 1H), 4.47 (s, 2H), 4.25 (d, *J* = 12.2 Hz, 1H), 4.15 (d, *J* = 12.2 Hz, 1H), 3.63 (dd, *J* = 7.6, 5.5 Hz, 1H), 3.40 (d, *J* = 7.6 Hz, 1H), 2.11 (s, 1H); ^{13}C NMR (100 MHz, $CDCl_3$): δ_{ppm} 174.8, 174.4, 135.31, 135.28, 134.5, 129.0, 128.4, 128.0, 92.1, 79.5, 61.4, 47.9, 46.0, 42.3; HRMS (ESI): Calc'd for $[M]^+$ ($C_{16}H_{15}NO_4$): 285.1001; Found: 285.1012. **3a-exo** ^{1}H NMR (600 MHz, $CDCl_3$): δ_{ppm} 7.33-7.26 (m, 5H), 6.61 (d, *J* = 5.7 Hz, 1H), 6.54 (dd, *J* = 5.7, 1.5 Hz, 1H), 5.28 (d, *J* = 1.7 Hz, 1H), 4.66 (s, 2H), 4.09 (dd, *J* = 12.2, 8.8 Hz, 1H), 4.03 (dd, *J* = 12.2, 6.3 Hz, 1H), 3.02 (d, *J* = 6.5 Hz, 1H), 2.99 (d, *J* = 6.5 Hz, 1H), 2.76 (bt, *J* = 7.4 Hz, 1H); ^{13}C NMR (100 MHz, $CDCl_3$): δ_{ppm} 175.7, 175.6, 138.3, 136.9, 135.2, 128.6, 128.0, 127.8, 91.4, 80.8, 60.7, 50.0, 48.1, 42.5; HRMS (ESI): Calc'd for $[M]^+$ ($C_{16}H_{15}NO_4$): 285.1001; Found: 285.0993.

Synthesis of compound 4a. Compound **3a** (500 mg, 1.75 mmol, 1.0 equiv.) was dissolved in

THF (10 mL). The resulting solution was then added dropwise into a phosgene solution (15 wt% in toluene, 3.8 mL, 5.25 mmol, 3.0 equiv.) under an argon atmosphere at room temperature and was stirred for 24 h. The residual phosgene and solvent were then removed under high vacuum to yield chloroformate **4a** (590 mg, 97%) as white gel. Phosgene collected in the liquid nitrogen-cooled trap was then quenched with methanol (20 mL) and saturated sodium hydroxide solution (20 mL). **Caution! Phosgene is highly toxic**. ^{1}H NMR (400 MHz, $CDCl_3$): δ_{ppm} 7.33-7.19 (m, 5H), 6.59 (dd, *J* = 5.5, 1.2 Hz, 2H), 6.44 (d, *J* = 5.5 Hz, 2H), 6.15 (dd, *J* = 5.9, 1.6 Hz, 1H), 5.98 (d, *J* = 5.9 Hz, 1H), 5.29 (d, *J* = 1.6 Hz, 2H), 5.26 (dd, *J* = 5.5, 1.6 Hz, 1H), 5.03-4.94 (m, 3H), 4.80-4.68 (m, 3H) 4.62 (s, 4H), 4.44 (s, 2H), 3.63 (dd, *J* = 7.8, 5.5 Hz, 1H), 3.34 (d, *J* = 7.8 Hz, 1H), 2.99-2.89 (m, 4H); ^{13}C NMR (100 MHz, $CDCl_3$): δ_{ppm} 174.9, 173.6, 150.5, 138.0, 135.9, 135.0, 128.9, 128.6, 127.9, 127.8, 125.2, 88.8, 81.2, 49.7, 48.4, 46.2, 42.3; HRMS (EI) calc'd. for $[M]^+$ ($C_{17}H_{14}ClNO_5$): 347.0561; Found: 347.0573.

Synthesis of compound 3b. *N*-propargyl maleimide[3] (1.70 g, 12.6 mmol, 1.0 equiv.) and 2-(hydroxymethyl)furan (1.1 mL, 1.24 g, 12.6 mmol, 1.0 equiv.) were dissolved in anhydrous acetonitrile (10 mL) under a nitrogen atmosphere in a flame-dried flask equipped with a magnetic stirring-bar. The reaction was stirred at 35 ºC for 14 hours. When TLC indicated the reaction had reached equilibrium, the solvent was removed, and the reaction was concentrated under reduced pressure for 1 h. NMR spectroscopy of the unpurified product indicated a ratio of (3.7:0.7:1.0) of endo-exo-unreacted maleimide. The crude material was then purified by flash chromatography (1:1 to 4:6 hexanes-ethyl acetate) to provide 2.09 g of a mixture of the endo and exo in an 80:20 ratio and a 72 % isolated yield. A small amount of material was purified further by preparative TLC (7:3 hexanes-ethyl acetate, 4 elutions) to provide analytical samples of both the endo and exo products. Due to the inherent thermal instability, the material is stored at -20 ºC until needed. **3b-endo** ^{1}H NMR (600 MHz, $CDCl_3$): δ_{ppm} 6.43 (dd, *J* = 5.8, 1.6 Hz, 1H), 6.31 (d, *J* = 5.8 Hz, 1H), 5.31 (dd, *J* = 5.5, 1.6 Hz, 1H), 4.26 (d, *J* = 12.8 Hz, 1H), 4.17 (d, *J* = 12.8 Hz, 1H), 4.06 (d, *J* = 2.5 Hz, 2H), 3.67 (dd, *J* = 7.6, 5.5 Hz, 1H), 3.48 (d, *J* = 7.6 Hz, 1H), 2.16 (t, *J* = 2.5 Hz, 1H), 2.10 (bs, 1H); ^{13}C NMR (100 MHz, $CDCl_3$): δ_{ppm} 173.8, 173.4, 135.6, 134.7,

92.3, 79.7, 76.0, 71.4, 61.4, 50.1, 48.2, 27.6; HRMS (ESI): Calc'd for $[M]^+$ ($C_{12}H_{11}NO_4$): 233.0688. Found: 233.06824. **3b-exo** ^{1}H NMR (400 MHz, $CDCl_3$): δ_{ppm} 6.62 (d, *J* = 5.7 Hz, 1H), 6.55 (dd, *J* = 5.7, 1.6 Hz, 1H), 5.29 (d, *J* = 1.7 Hz, 1H), 4.25 (d, *J* = 2.5 Hz, 2H), 4.10 (d, *J* = 1.8 Hz, 2H), 3.68 (dd, *J* = 7.6, 5.5 Hz, 1H), 3.48 (d, *J* = 7.6 Hz, 1H), 2.21 (t, *J* = 2.5, 2.5 Hz, 1H), 1.64 (bs, 1H); ^{13}C NMR (100 MHz, $CDCl_3$): δ_{ppm} 174.5, 174.4, 138.3, 137.0, 91.5, 80.9, 76.2, 71.7, 60.5, 50.1, 48.1, 27.9; ESI (MS): Calc'd for $[M]^+$ ($C_{12}H_{11}NO_4$): 233.0688; Found: 233.06892.

Synthesis of compound 4b. Compound **3b** (500 mg, 2.15 mmol, 1.0 equiv.) was dissolved in THF (10 mL). The resulting solution was then added dropwise into a phosgene solution (15 wt% in toluene, 4.6 mL, 6.44 mmol, 3.0 equiv.) under an argon atmosphere at room temperature and was stirred for 24 h. The residual phosgene and solvent were then removed by high vacuum to yield chloroformate **4b** (610 mg, 97%) as a white gel. Phosgene collected in the liquid nitrogen-cooled trap was then quenched with methanol (20 mL) and saturated sodium hydroxide solution (20 mL). **Caution! Phosgene is highly toxic.** ^{1}H NMR (600 MHz, $CDCl_3$): δ_{ppm} 6.66 (d, *J* = 5.3 Hz, 2 H), 6.53 (d, *J* = 5.3 Hz, 1 H), 6.50 (d, *J* = 5.9 Hz, 2 H), 6.34 (d, *J* = 5.9 Hz, 1 H), 5.39 (d, *J* = 4.1 Hz, 1H), 5.35 (s, 2 H), 5.09-5.05 (m, 3 H), 4.88 (d, *J* = 12.3 Hz, 1H), 4.78 (d, *J* = 12.9 Hz, 2H), 4.25 (d, *J* = 2.9 Hz,4 H), 4.11 (d, *J* = 2.4 Hz, 3 H), 3.73 (dd, *J* = 5.3, 2.4 Hz, 1H), 3.46 (d, *J* = 7.6 Hz, 1H), 3.08 (d, *J* = 6.5 Hz, 2 H), 3.00 (d, *J* = 6.5 Hz, 2 H), 2.21 (t, *J* = 2.4 Hz, 1H), 2.19 (t, *J* = 2.4 Hz, 1H); ^{13}C NMR (150 MHz, $CDCl_3$): δ_{ppm} 174.0, 172.8, 150.9, 138.4, 136.4, 133.7, 129.2, 128.4, 125.5, 89.3, 81.5, 76.2, 71.9, 68.1, 50.2, 48.8, 46.7, 28.3, 27.9; HRMS (EI) calc'd. for $[M]^+$ $C_{13}H_{10}ClNO_5$: 295.0248; Found: 295.0257.

Synthesis of PEtG-DA-Bn and typical procedure for synthesis of end-capped PEtG. Ethyl glyoxylate in toluene solution (20.0 mL) was distilled under vacuum (25 °C, 0.3 mbar) over P_2O_5 to remove toluene and trace water in the first, discarded fraction. The residue was then distilled twice successively over P_2O_5 at atmospheric pressure under argon at 130 °C to obtain the highly pure monomer. Purified ethyl glyoxylate (2.0 mL, 20 mmol, 1.0 equiv.) was dissolved in CH_2Cl_2 (2.0 mL) and Et_3N (1.4 μL, 10 μmol, 0.0005 equiv.) was added. The solution was stirred for 1 h at

-20 ˚C. Compound **4a** (0.1 g, 280 μmol, 0.014 equiv.) and Et_3N (38 μL, 280 μmol, 0.014 equiv.) were added at -20 °C to end-cap the polymer. The solution was gradually warmed to room temperature and then stirred for 16 h. Purification was achieved by precipitation of the crude reaction mixture into methanol. After decanting the excess methanol, the residue was dried *in vacuo* to provide 1.1 g of a white, sticky polymer in 55% yield. ^{1}H NMR (600 MHz, $CDCl_3$): δ 7.28-7.32 (m, 10 H), 5.48-5.73 (m, 239 H), 4.15-4.31 (m, 449 H), 1.23-1.36 (m, 658 H). FT-IR: 2985, 1748, 1468, 1447, 1376, 1297, 1214, 1137, 1094, 1015, 989, 856, 675 cm^{-1}. SEC: M_n = 33 kg/mol, M_w = 59 kg/mol, $Đ$ = 1.8.

Synthesis of PEtG-DA-alkyne. The polymer is synthesized by the same procedure described for **PEtG-DA-Bn** except that compound **4b** was used as the end-cap. The yield was 60%. ^{1}H NMR (600 MHz, $CDCl_3$): δ 5.47-5.76 (m, 630 H), 4.14-4.29 (m, 1184 H), 1.24-1.40 (m, 1754 H). FTIR: 2985, 1748, 1468, 1447, 1376, 1297, 1214, 1138, 1094, 1016, 962, 857, 675 cm^{-1}. SEC: M_n = 63 kg/mol, M_w = 130 kg/mol, $Đ$ = 2.0.

Synthesis of Block Copolymer PEtG-DA-PEG750. 750 g/mol PEG-N_3 (36.0 mg, 48 μmol, 6 equiv.) and **PEtG-DA-alkyne** (500.0 mg, 8 μmol, 1 equiv.) were dissolved in DMF (5.0 mL). After removing the air and refilling with argon, $CuSO_4$ (4.0 mg, 28 μmol, 3.5 equiv.) and sodium ascorbate (5.0 mg, 28 μmol, 3.5 equiv.) were added into the solution, and the mixture was stirred at 40 ˚C for 16 h. The reaction mixture was then transferred into a regenerated cellulose membrane (50 kg/mol MWCO) and dialyzed against deionized water for 16 h (1 L, 2 solvent changes) to remove DMF and most free PEG. The dialyzed material was then lyophilized, washed 3 times with water to further remove free PEG, and then dried to afford 500 mg of the product as a white, rubber-like, polymer in 98% yield. ^{1}H NMR (600 MHz, $CDCl_3$): δ 5.47-5.75 (m, 341 H), 4.07-4.33 (m, 704 H), 3.63 (s, 136 H), 3.37 (s, 6 H), 1.13-1.42 (m, 1075 H). ^{13}C NMR (150 MHz, $CDCl_3$): δ 164.7-166.3, 90.3-94.7, 70.7, 62.3, 14. FTIR: 2985, 1750, 1468, 1447, 1376, 1298, 1216, 1138, 1017, 1095, 964, 857, 677 cm^{-1}. SEC: M_n = 59 kg/mol, M_w = 111 kg/mol, $Đ$ = 1.9.

Synthesis of PEtG-DA-PEG5000. The polymer was synthesized by the same procedure described above for the synthesis of **PEtG-DA-PEG750**, except that 5000 g/mol PEG-N_3 was used. The yield was 98 %. ^{1}H NMR (600 MHz, $CDCl_3$): δ 5.45-5.70 (m, 670 H), 4.10-4.30 (m, 1399 H), 3.62 (s, 909 H), 3.36 (s, 3 H), 1.20-1.34 (m, 2110 H). ^{13}C NMR (150 MHz, $CDCl_3$): δ 164.6-166.7, 90.8-93.9, 70.5, 62.0, 13.8. FT-IR (thin film): 2985, 2874, 1750, 1468, 1448, 1376, 1298, 1216, 1136, 1095, 1018, 962, 856, 680 cm^{-1}. SEC: M_n = 35 kg/mol, M_w = 71 kg/mol, $Đ$ = 2.0.

Synthesis of Vesicle-control. The polymer was synthesized by the same procedure as **Micelle-control**[1a], except that 750 g/mol PEG-N_3 was used. The yield was 86%. ^{1}H NMR (600 MHz, $CDCl_3$): δ 5.47-5.77 (m, 553 H), 4.07-4.36 (m, 1040 H), 3.65 (s, 136 H), 3.39 (s, 9 H), 1.13-1.47 (m, 1573 H). ^{13}C NMR (150 MHz, $CDCl_3$): δ 164.0-166.5, 90.0-94.2, 70.5, 62.0, 13.8. FT-IR (thin film): 2985, 2874, 1752, 1467, 1448, 1376, 1297, 1217, 1140, 1096, 1018, 965, 855, 732 cm^{-1}. SEC: M_n = 77 kg/mol, M_w = 177 kg/mol, $Đ$ = 2.3.

Study of PEtG-DA-Bn Depolymerization in Solution and Representative Procedure for Studying Depolymerization by NMR Spectroscopy. PEtG-DA-Bn (15.0 mg) was dissolved in a 9:1 mixture of CD_3CN: D_2O (1.2 mL) at ambient temperature (22 °C). The solution was then divided between two NMR tubes. One tube was incubated at 75 °C in an oven, while the other one was stored at room temperature (22 °C). ^{1}H NMR spectra were recorded at defined intervals to monitor the depolymerization of the materials. At the same time, benzyl chloroformate end-capped PEtG (**PEtG-control**)[1b] was also subjected to the same procedure and its depolymerization was monitored by NMR spectroscopy as non-triggerable control. The extent of depolymerization was calculated as % depolymerization = 100 – x, where x is the integration of the peak at 5.5 ppm, when the integration of the peak at 4.2 ppm was set to 200 (which remained constant as it corresponds to the *$CH_3\underline{CH_2}O$*- in both polymer and the depolymerization product).

Self-assembly of PEtG-PEG Block Copolymers. 8.0 mg of block copolymer was fully dissolved in 1.0 mL of organic solvent by stirring overnight (THF for **PEtG-DA-PEG750** and

Vesicle-control and DMSO for **PEtG-DA-PEG5000** and **Micelle-control**). For vesicles, 0.9 mL deionized water was added slowly into 0.1 mL of copolymer in THF with gentle stirring. For micelles, 0.1 mL of the copolymer in DMSO was injected quickly into 0.9 mL of rapidly stirring deionized water. After stirring for 10 minutes, the suspension was then dialyzed against deionized water for 16 h (1 L, 2 solvent changes) to remove THF or DMSO, affording an aqueous suspension of assemblies.

Study of Assembly Decomposition by DLS. The assemblies were formed by the procedure described above, except that the assemblies suspension was dialyzed against 100 mM pH 7.4 phosphate buffer solution. The assemblies were then transferred into plastic cuvettes and the CR was measured by DLS while fixing the attenuator. Samples were then incubated either at 75 °C in an oven or at room temperature (22 °C). CR changes were recorded at defined intervals to monitor the decomposition of assemblies.

Study of Nile Red Release.

A stock of copolymer assembly solution at a concentration of 0.8 mg/mL was prepared by the above standard self-assembly procedure in pH 7.4 phosphate buffer. 29 μL of a 0.1 mg/mL solution of Nile red in CH_2Cl_2 was added to each of a series of vials and then the solvent was evaporated to provide a thin film of Nile red. To each vial, 1.5 mL of assembly suspension was added, and the vials were gently shaken for 16 h to incorporate Nile red into the nanoparticles. After the initial fluorescence emission (600 nm) of the micelle suspension was measured using an excitation wavelength of 540 nm. Some samples were stored in an oven at 75 °C, with others were stored at room temperature (22 °C). The fluorescence emission was recorded at defined intervals to monitor the decomposition of assemblies.

Study of Assembly Depolymerization by ^{1}H NMR Spectroscopy. 10.0 mg of block copolymer was fully dissolved in 0.4 mL of DMSO-d_6. 0.2 mL of the resulting solution was rapidly injected into 1.0 mL of 100 mM, pH 7.4 phosphate buffered D_2O. After stirring for 10 min, the micelle suspension was divided between two NMR tubes. One tube was incubated in an oven at 75 °C,

while the other one was kept at room temperature. ^{1}H NMR spectra were recorded at defined intervals to monitor the depolymerization of the materials. At the same time, **Micelle-control** was subjected to the same procedure. Percent depolymerization was determined using the sum of the integration of the methyl peaks corresponding to EtGH and ethanol (1.0-1.2 ppm), which plateaued at a very similar (1872) value to that of the methyl peak at 1.17-1.45 ppm in the block copolymer taken in $CDCl_3$ (integration 2111) when setting the PEG peak integral to 909. The % polymer remaining was calculated as 100 - (sum of integration from 1.0-1.2 ppm/1872))×100.

"Polyol" Synthesis of Iron Oxide Nanoparticles[4]. 1.082 g (4.0 mmol) of $FeCl_3.6H_2O$ and 398 mg (2.0 mmol) of $FeCl_2.4H_2O$ were dissolved in a mixture of 40 g of di(ethylene glycol) (DEG) and 40 g of *N*-methyldiethanolamine (NMDEA). Meanwhile, 640 mg (16 mmol) of NaOH was dissolved in a mixture of 20 g of DEG and 20 g of NMDEA. Both solutions were stirred overnight under nitrogen flux to prevent the oxidation of Fe^{2+} species. The solutions were then mixed and stirred for 3 h, before heating the mixture to 210 °C with an oil bath, reflux set-up and mechanical agitation. The set-up was open and a flux of nitrogen helped to remove traces of water before temperature reaches 210 °C. Once a temperature of 210 °C was reached, the set-up was closed, and 1 mL of water was injected in the system with a syringe through a septum, leading to a burst of nuclei. The formation of nanoparticles was carried on for 30 min, then the system was cooled to room temperature. The black sediment was separated magnetically and washed with a mixture of ethanol and ethyl acetate (1:1 v/v) 3 times. Possible iron hydroxides were removed by treatment with 10% nitric acid. The nanoparticles were then washed 2 times with acetone and 2 times with diethyl ether before being dispersed in water.

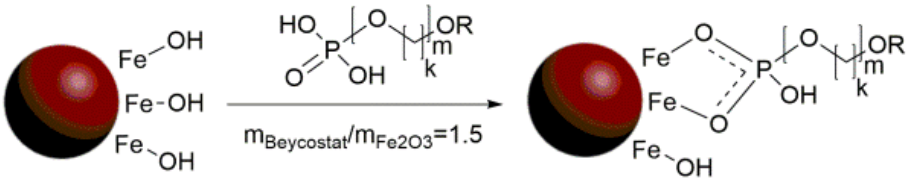

Scheme S2. Coating of IONPs.

Coating of IONPs. 113 mg of Beycostat NE was deposited in a 50 mL beaker. 15.0 mL of water was added and the solution was stirred with a mechanical agitator. 2.5 mL of a ferrofluid with an iron oxide concentration of 18.0 g/L (45 mg of iron oxide in solution) was added to the surfactant. Then 2.6 mL of a 69 % w/w HNO_3 solution was added to reach a final HNO_3 concentration of 2.0 M. The solution was heated to 60 °C for 30 min with a water bath. The nanoparticles were then sedimented over a permanent magnet and washed 3 times with 50 mL of methanol, before being dispersed in 45 mL of dichloromethane or tetrahydrofuran (THF). The iron oxide content of this dispersion was estimated by dissolving 50.0 microliters of solution in 5.0 mL of 5.0 M HCl M with the help of a sonication bath. The absorption at 350 nm correspondng to the peak of the $[Fe(Cl)_6]^{3-}$ complex was compared to a calibration curve. The final concentration was estimated at 6.0 g/L of Fe_2O_3.

Loading of IONPs into Micelles. 1.0 mg of **PEtG-DA-PEG5000** or **Micelle-control** was dissolved in 0.2 mL of THF, meanwhile IONPs (dispersed in THF with a concentration of 6.0 mg/mL) were mixed at different feed weight ratios (FWR) as needed with the polymer solution. This mixture was then added dropwise to 1.8 mL water via a micro-syringe while magnetically stirring. THF was allowed to evaporate by leaving the vials open for 24 h.

Dynamic Light Scattering Coupled with Magnetic Field Hyperthermia. The combined DLS-MFH set-up based on a remote DLS setup VASCO Flex™ from Cordouan Technologies (Pessac, France) has been previously reported[5] and is shown in Fig. S40. Micelles loaded with 35 mass % IONPs were studied by DLS-MFH. The sample was heated up to the desired external temperature by a water bath. The temperature of the sample was measured with an optical fiber probe. After 1 h equilibration at the target temperature, the alternating magnetic field was applied at the maximum available amplitude of 10.2 kA/m and frequency of 755 kHz. Meanwhile, DLS was operating continuously at a backscattering angle of 165° to measure the sample diameter (Z-average), polydispersity index (PDI) and signal intensity changes during this period.

Small angle neutron scattering (SANS) experiments were performed at the Orphée neutron

facility of LLB-CEA (Saclay, France) on the PAXY spectrometer equipped with a 2D (anisotropic SANS) detector. Micelles were suspended at a concentration of 0.6 $mg \cdot mL^{-1}$ in pure D_2O, of neutron scattering length density $SLD(D_2O)=6.40\times10^{-6}$ $Å^{-2}$. The calculated SLD of iron oxide and ethyl glyoxylate monomer are $SLD(\gamma\text{-}Fe_2O_3)=6.98\times10^{-6}$ $Å^{-2}$ and $SLD(EtG)=1.31\times10^{-6}$ $Å^{-2}$, respectively. The neutron scattering contrast of the micelles in heavy water thus arises almost exclusively from the hydrophobic Poly(EtG) block of the polymer, the hydrophilic PEG block being highly hydrated, thus having negligible contribution to the neutron scattering contrast. Three beamline configurations were used to cover overlapping scattering vector (q) ranges of $1.92\times10^{-3} – 2.84\times10^{-2}$, $1.05\times10^{-2} – 0.154$, and $3.19\times10^{-2} – 0.427$ $Å^{-1}$, with the following values of sample-to-detector distance D and neutron wavelength λ: D=7 m and λ=15 Å, D=3 m and λ=6 Å, D=1 m and λ=6 Å. The scattering intensity curves were divided by the transmission factor and subtracted from the incoherent background, before normalizing by the flat signal of a cuvette filled with light water to correct the detector efficiency, yielding the absolute intensity in cm^{-1}.

3. NMR Spectra of compounds and polymers

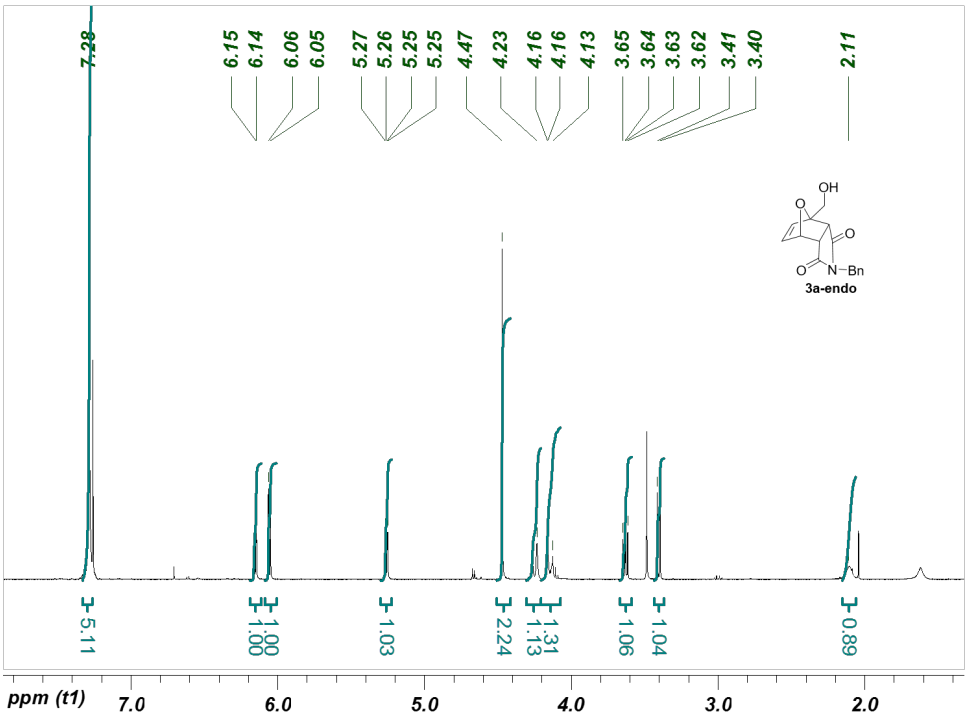

Figure S1. ^{1}H NMR spectrum of Compound **3a-endo** ($CDCl_3$, 600Hz).

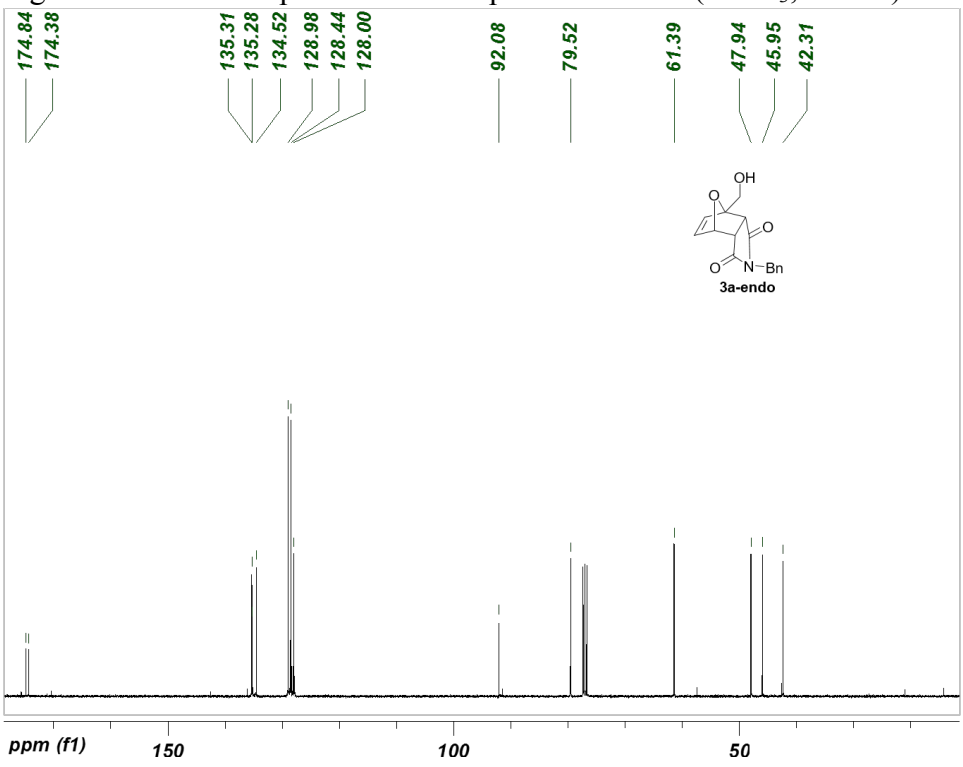

Figure S2. ^{13}C NMR spectrum of Compound **3a-endo** ($CDCl_3$, 100Hz).

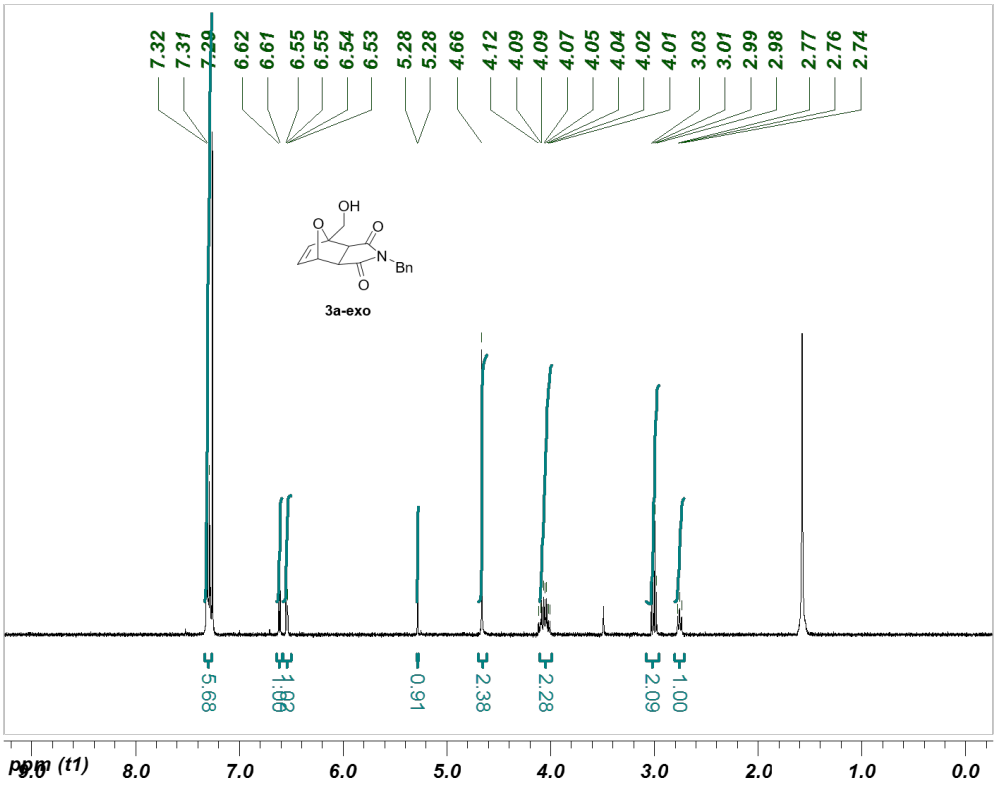

Figure S3. ^{1}H NMR spectrum of Compound **3a-exo** ($CDCl_3$, 600Hz)

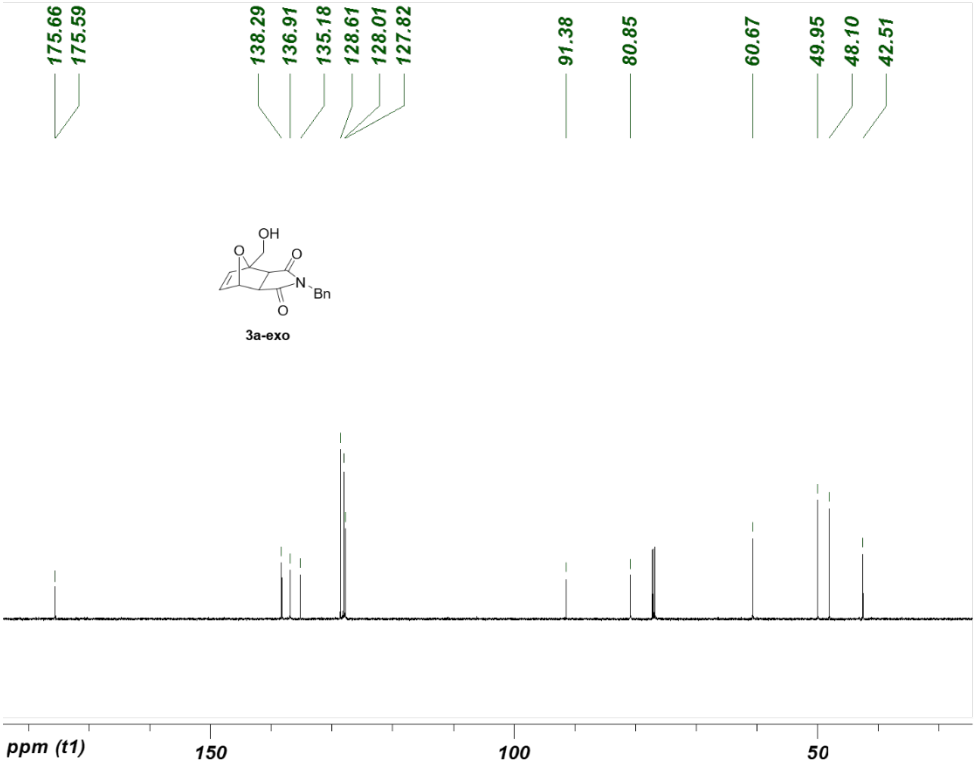

Figure S4. ^{13}C NMR spectrum of Compound **3a-exo** ($CDCl_3$, 100Hz).

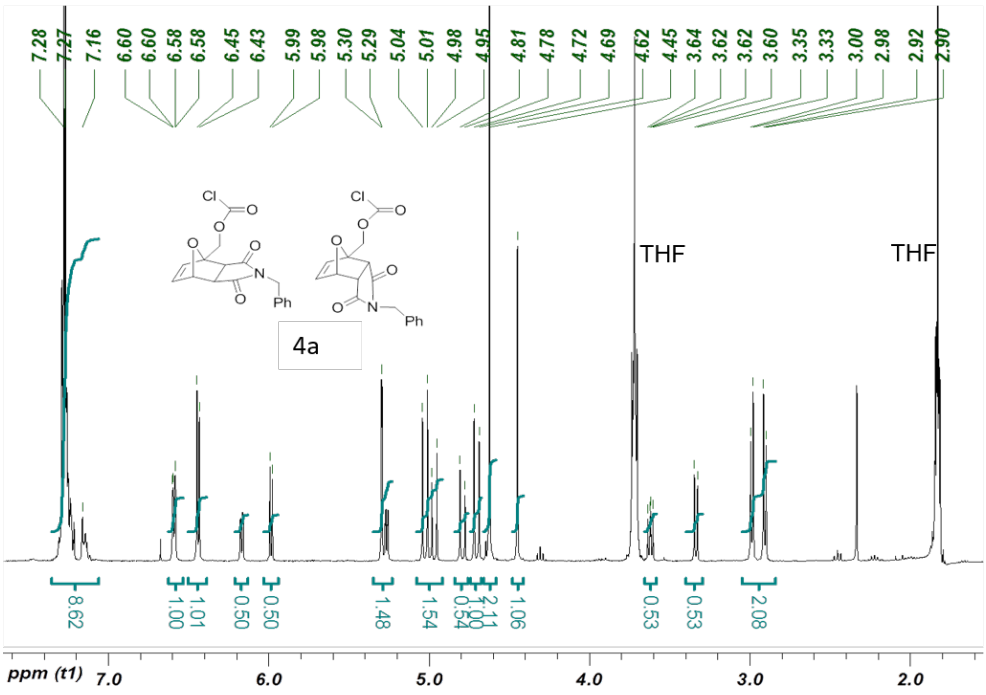

Figure S5. ^{1}H NMR spectrum of Chloroformate **4a** ($CDCl_3$, 400Hz) (residual THF present).

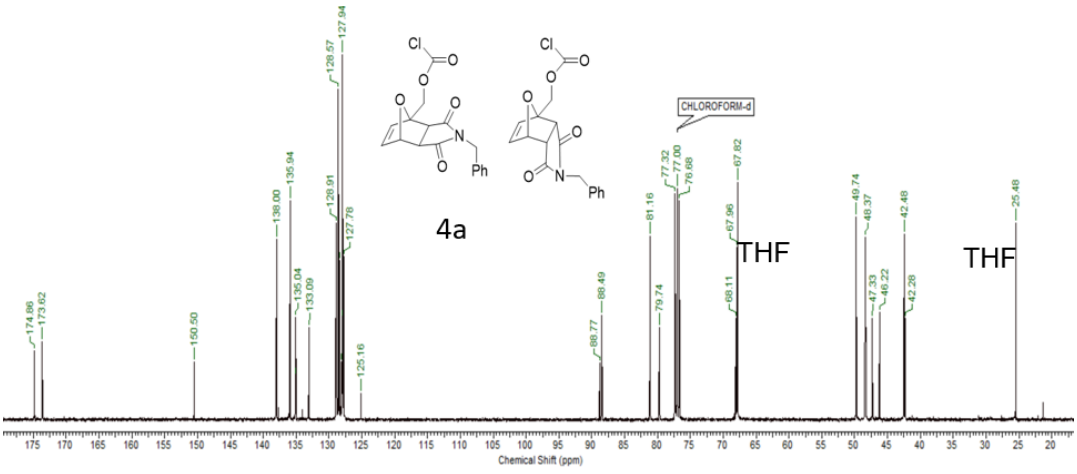

Figure S6. ^{13}C NMR spectrum of Chloroformate **4a** ($CDCl_3$, 100Hz).

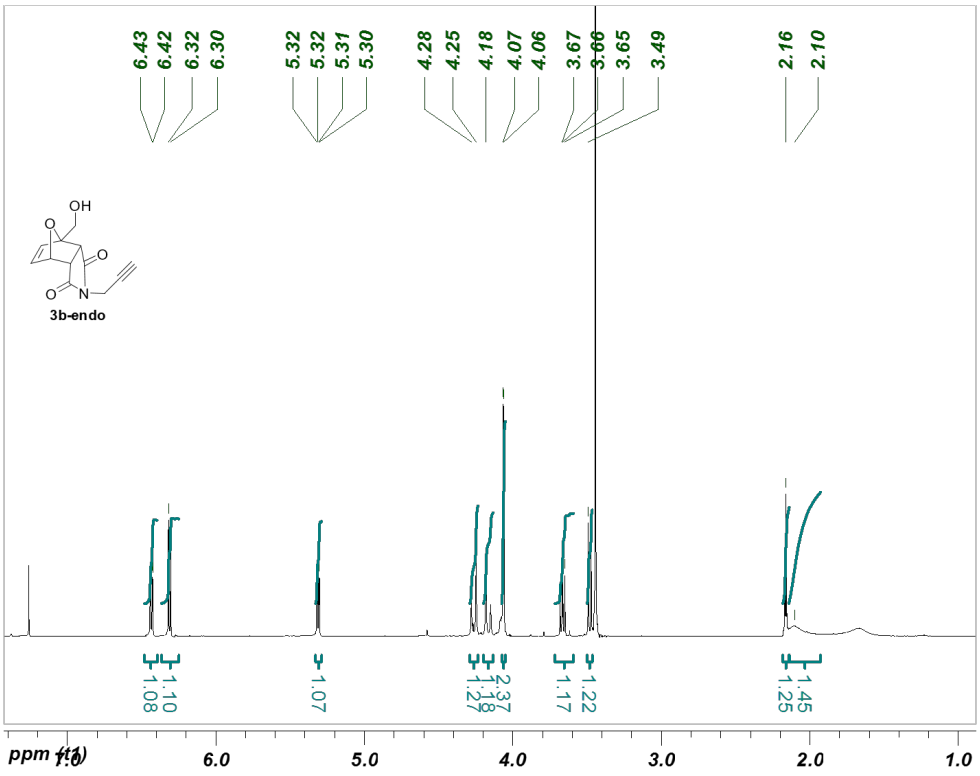

Figure S7. ^{1}H NMR spectrum of Compound **3b-endo** ($CDCl_3$, 600Hz).

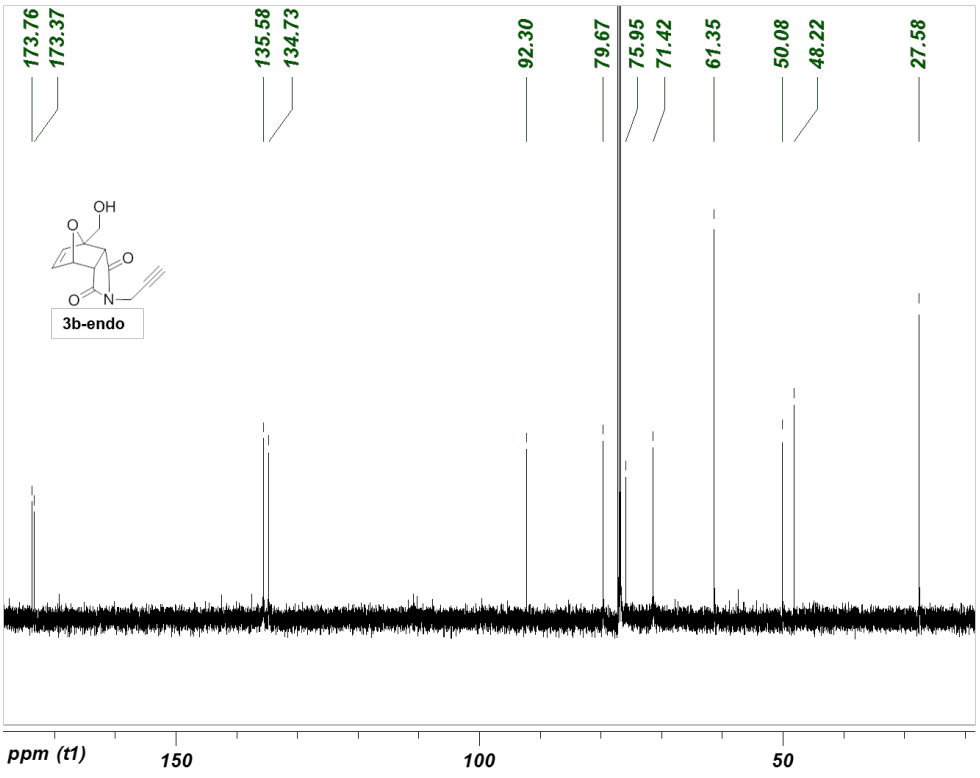

Figure S8. ^{13}C NMR spectrum of Compound **3b-endo** ($CDCl_3$, 100Hz).

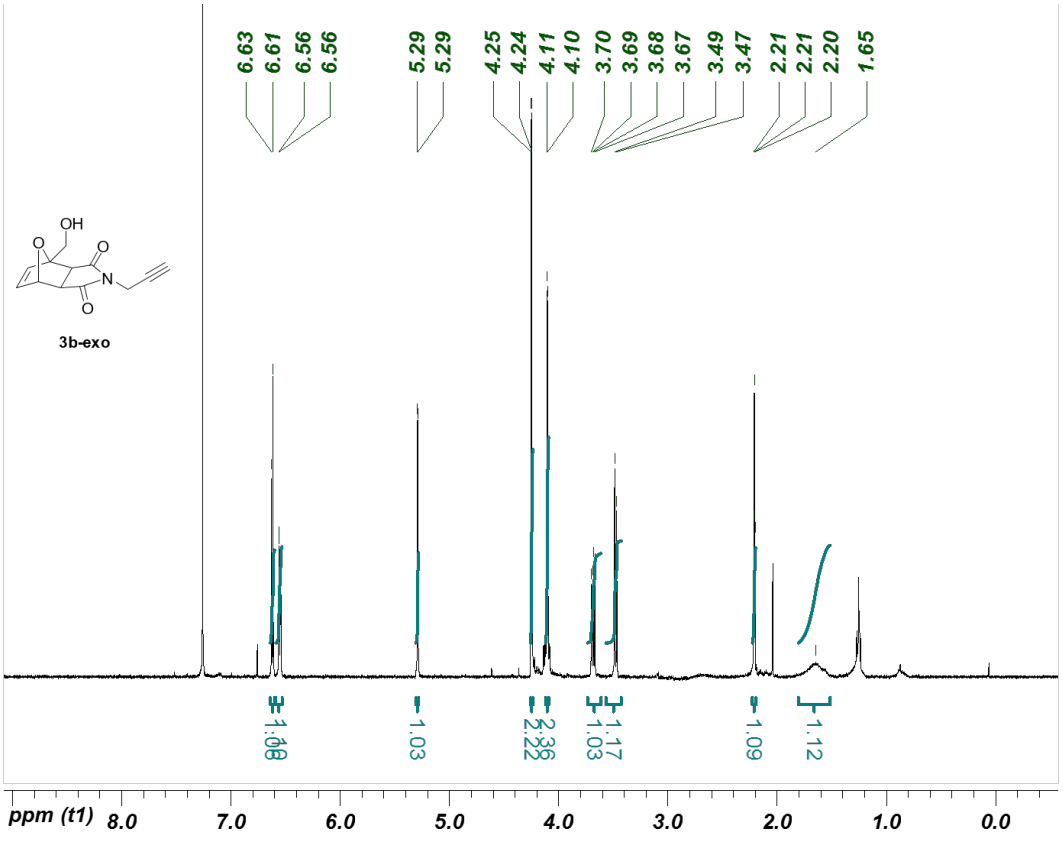

Figure S9. ^{1}H NMR spectrum of Compound **3b-exo** ($CDCl_3$, 400Hz).

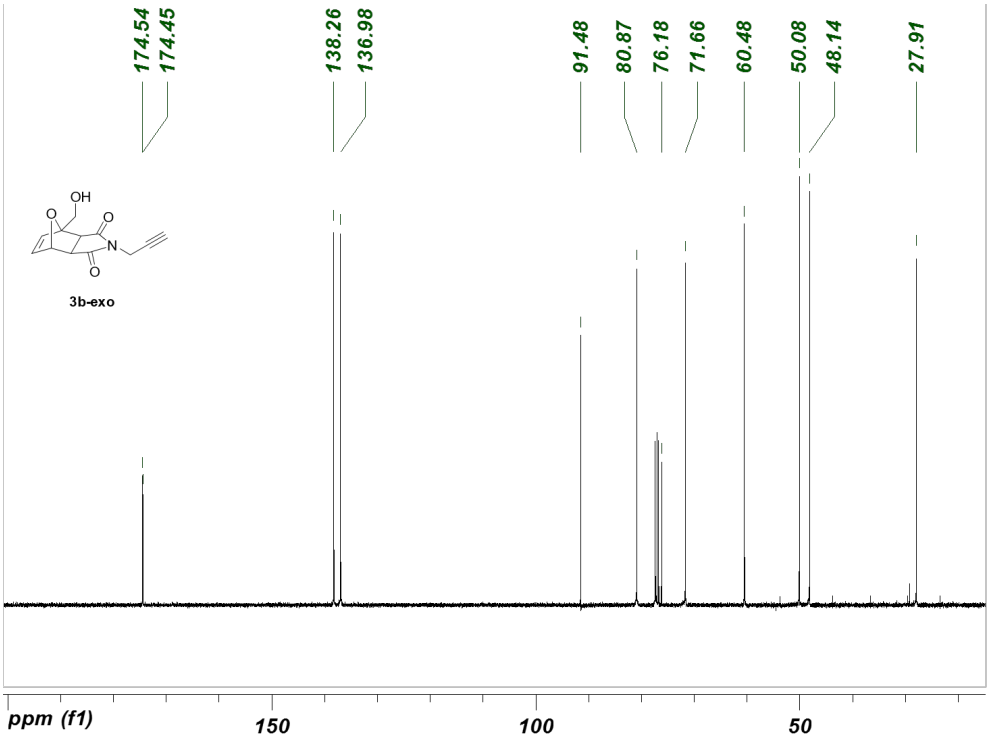

Figure S10. ^{13}C NMR spectrum of Compound **3b-exo** ($CDCl_3$, 100Hz).

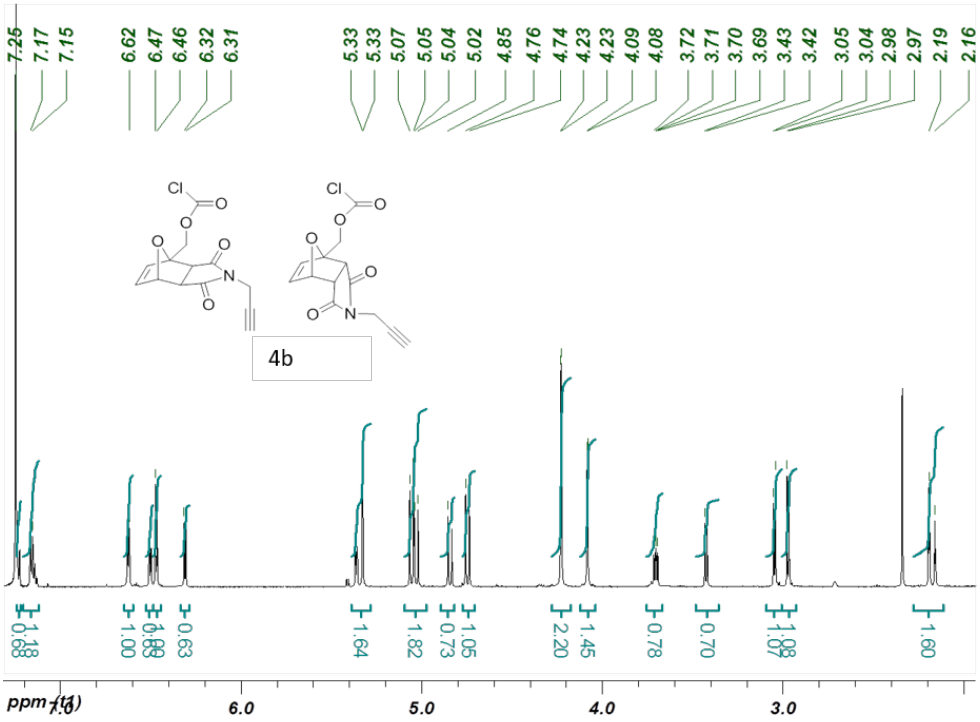

Figure S11. ^{1}H NMR spectrum of Chloroformate **4b** ($CDCl_3$, 400Hz).

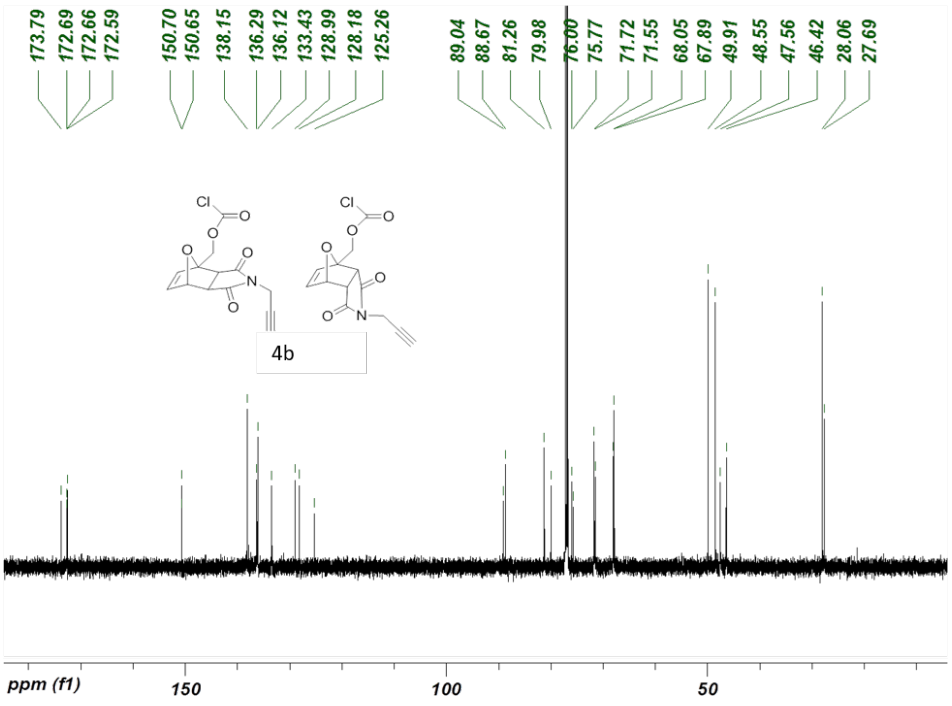

Figure S12. ^{13}C NMR spectrum of Chloroformate **4b** ($CDCl_3$, 100Hz).

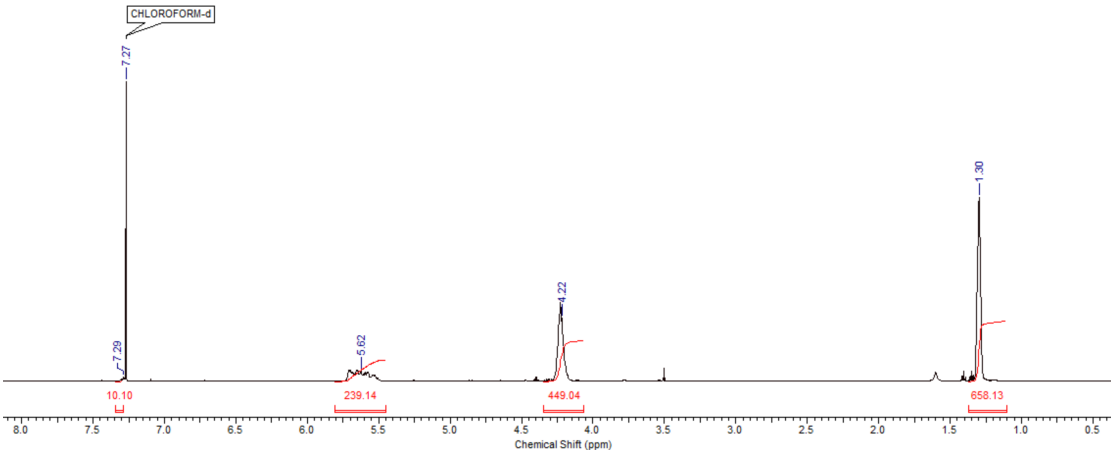

Figure S13. ^{1}H NMR spectrum of **PEtG-DA-Bn** ($CDCl_3$, 600Hz).

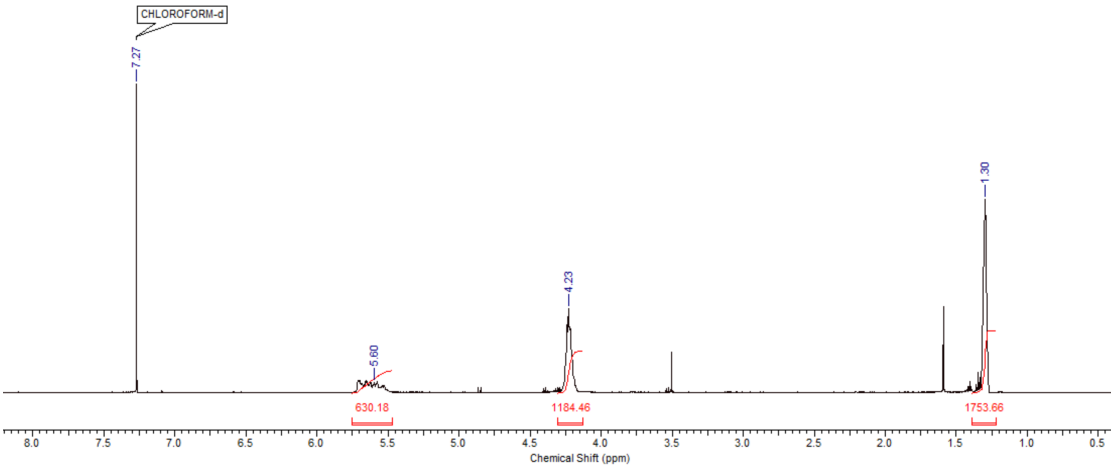

Figure S14. ^{1}H NMR spectrum of **PEtG-DA-alkyne** ($CDCl_3$, 600Hz).

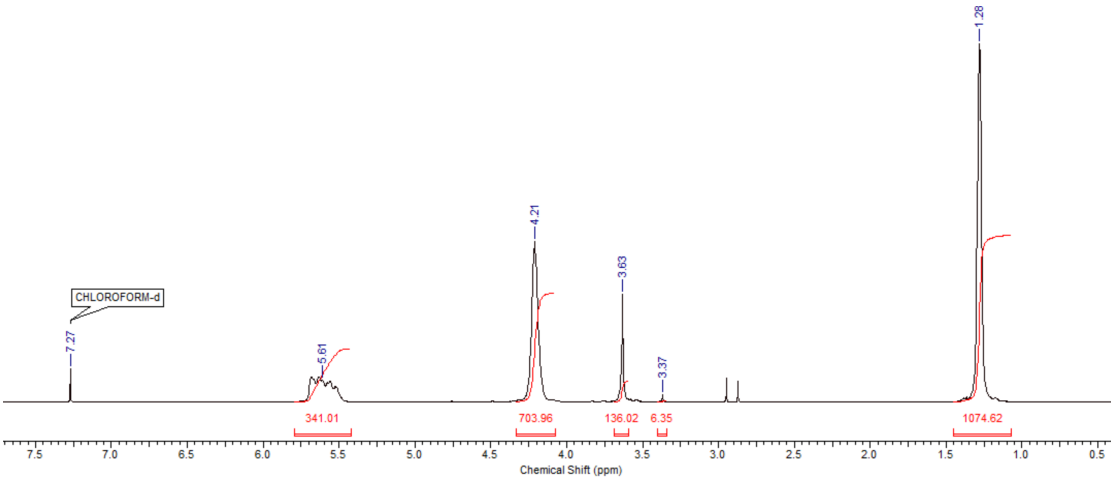

Figure S15. ^{1}H NMR spectrum of **PEtG-DA-PEO750** ($CDCl_3$, 600Hz). The success of the PEG coupling is evidenced by the presence of the PEG peak at 3.6 ppm and its corresponding integration.

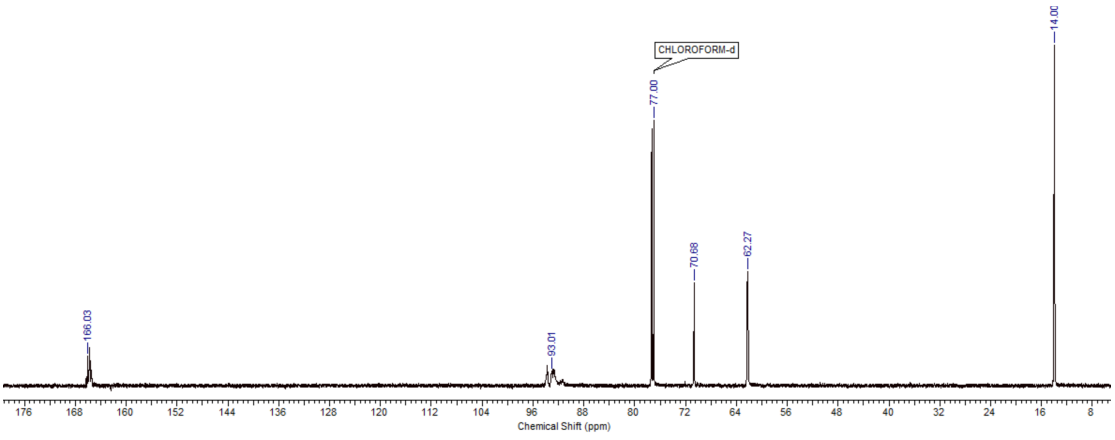

Figure S16. ^{13}C NMR spectrum of **PEtG-DA-PEO750** ($CDCl_3$, 150Hz). The success of the PEG coupling is evidenced by the presence of the PEG peak at 70 ppm.

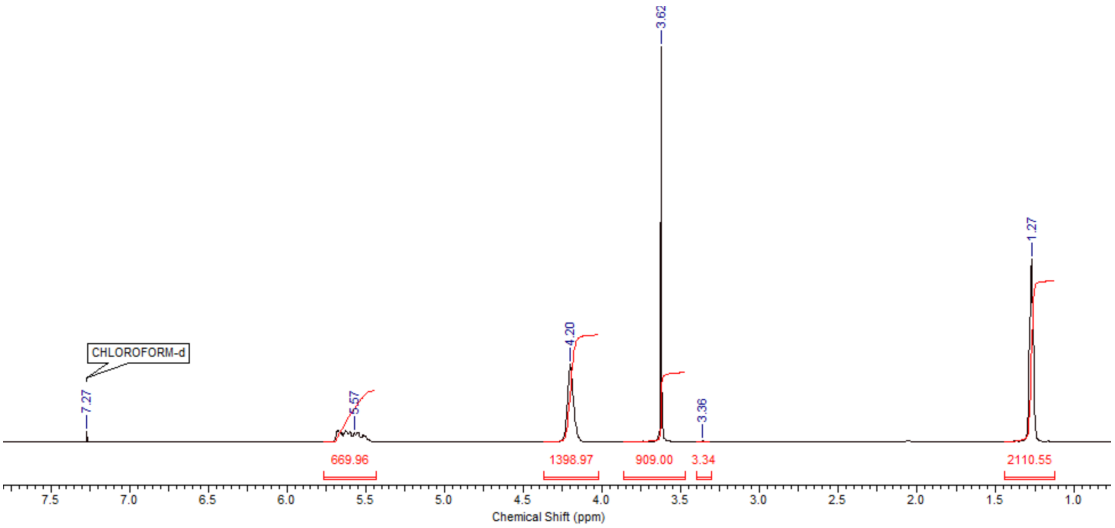

Figure S17. ^{1}H NMR spectrum of **PEtG-DA-PEO5000** ($CDCl_3$, 600Hz). The success of the PEG coupling is evidenced by the presence of the PEG peak at 3.6 ppm and its corresponding integration.

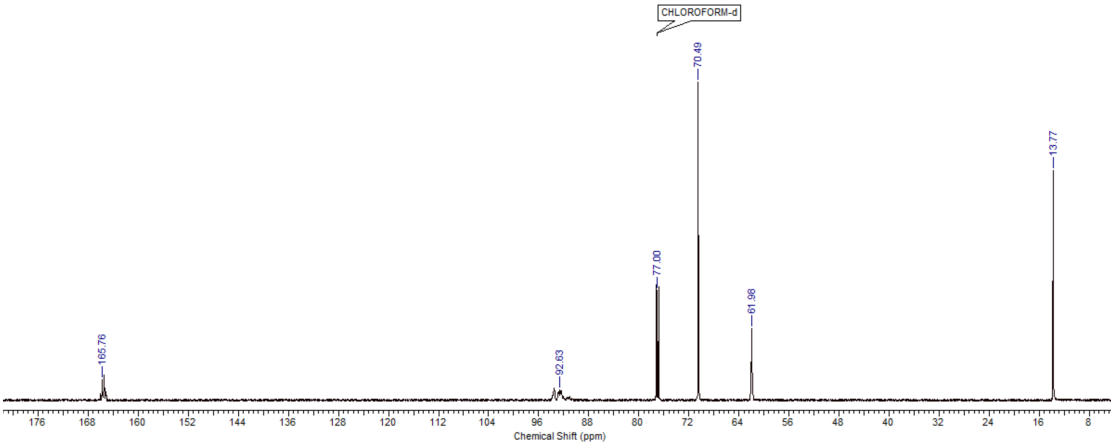

Figure S18. ^{13}C NMR spectrum of **PEtG-DA-PEO5000** ($CDCl_3$, 150Hz). The success of the PEG coupling is evidenced by the presence of the PEG peak at 70 ppm.

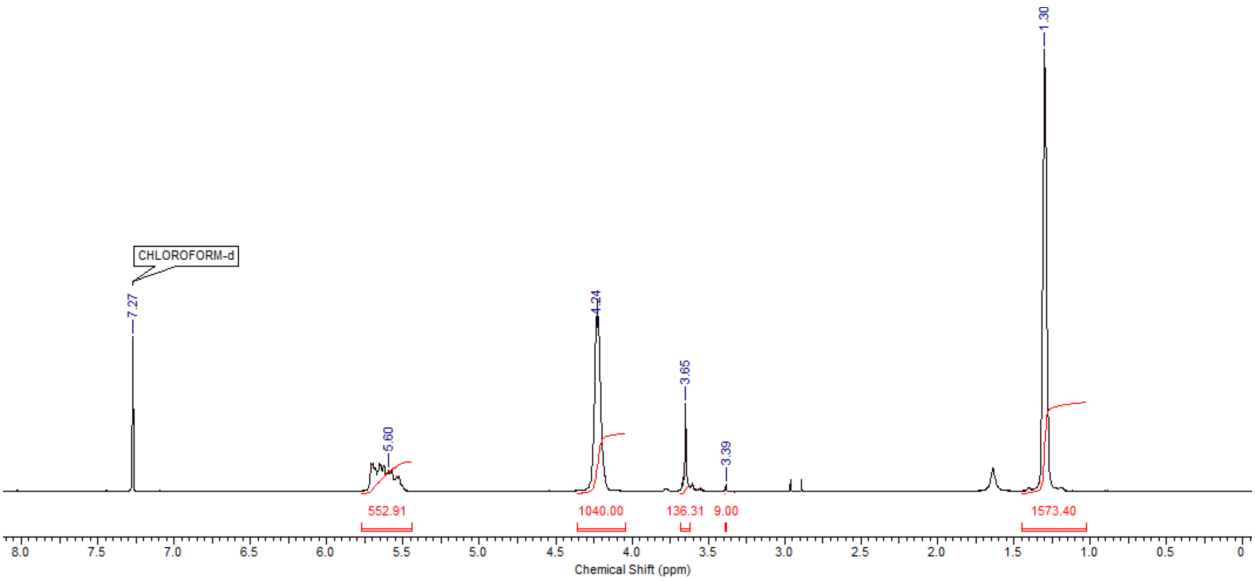

Figure S19. ^{1}H NMR spectrum of **Vesicle-control** ($CDCl_3$, 600Hz). The success of the PEG coupling is evidenced by the presence of the PEG peak at 3.6 ppm and its corresponding integration.

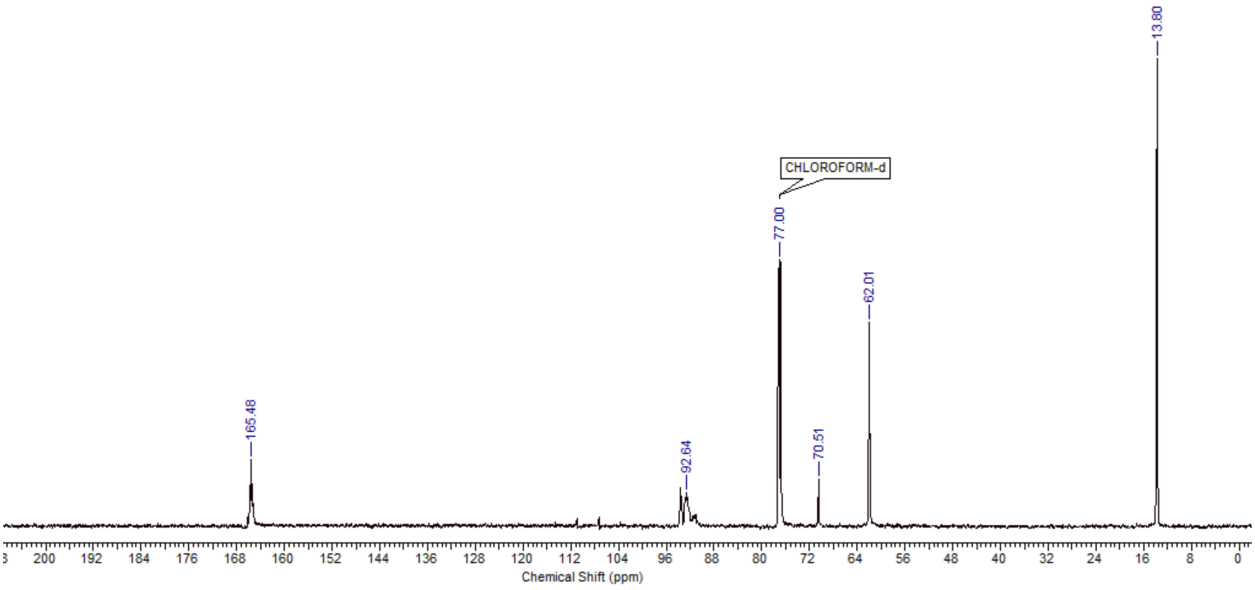

Figure S20. ^{13}C NMR spectrum of **Vesicle-control** ($CDCl_3$, 150Hz). The success of the PEG coupling is evidenced by the presence of the PEG peak at 70 ppm.

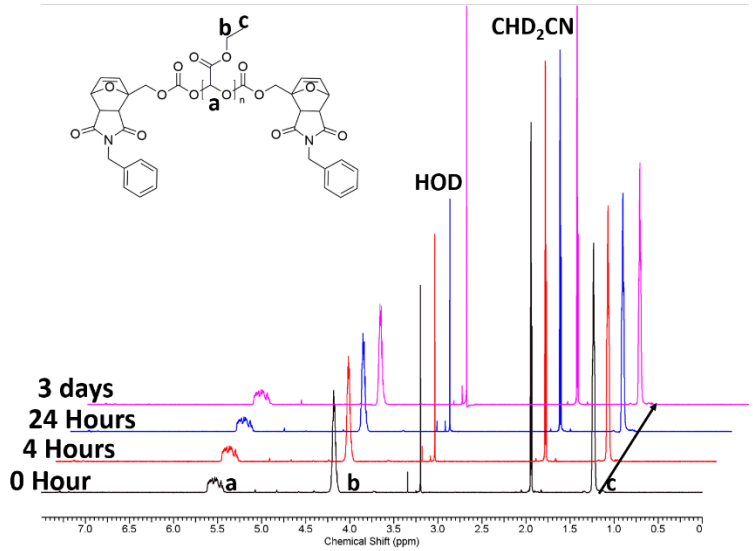

Figure S21. ^{1}H NMR spectra of **PEtG-DA-Bn** incubated in 9:1 CD_3CN:D_2O at 22 °C over time. Spectra are offset to allow the progression over time to be clearly observed.

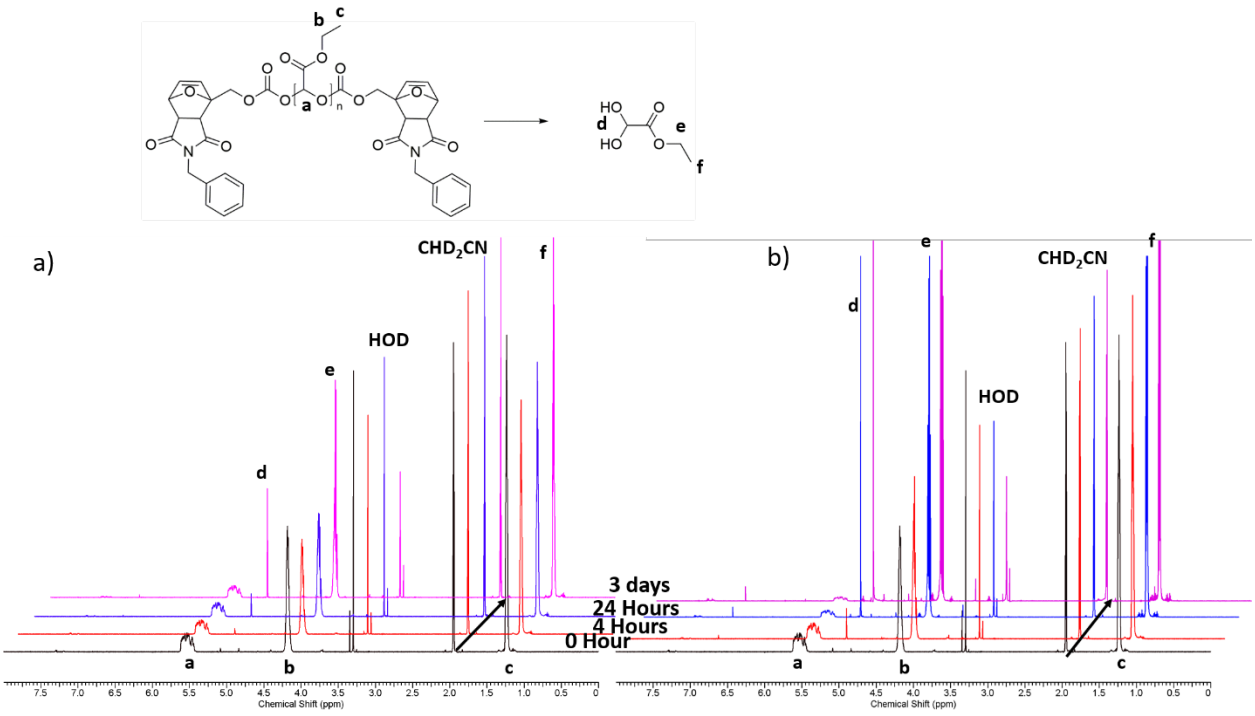

Figure S22. ^{1}H NMR spectra of **PEtG-DA-Bn** incubated in 9:1 CD_3CN:D_2O at a) 40 °C and b) 60 °C. Spectra are offset to allow the progression over time to be clearly observed.

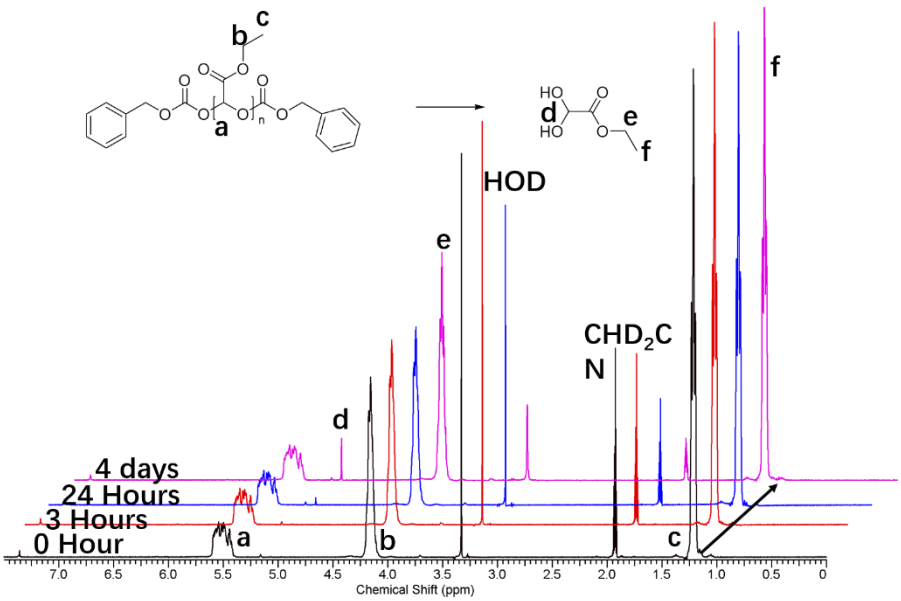

Figure S23. ^{1}H NMR spectra of **PEtG-control** incubated in 9:1 CD_3CN:D_2O at 75 °C. Spectra are offset to allow the progression over time to be clearly observed.

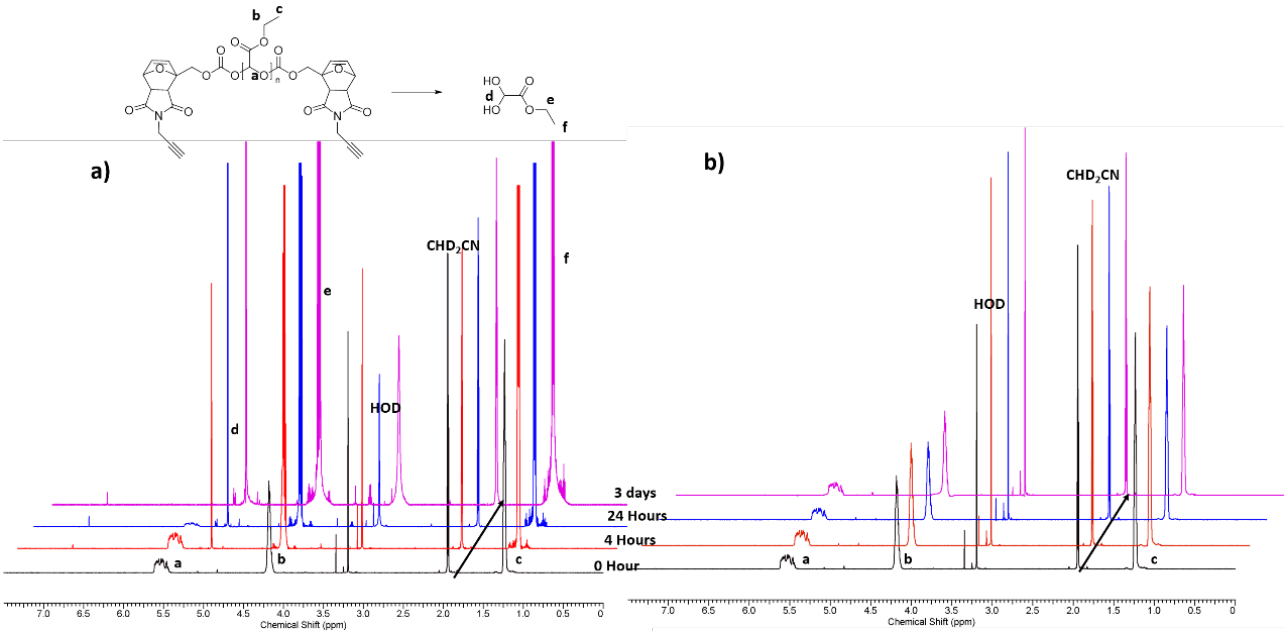

Figure S24. ^{1}H NMR spectra of **PEtG-DA-alkyne** incubated in 9:1 CD_3CN:D_2O at a) 75 °C and b) 22 °C. Spectra are offset to allow the progression over time to be clearly observed.

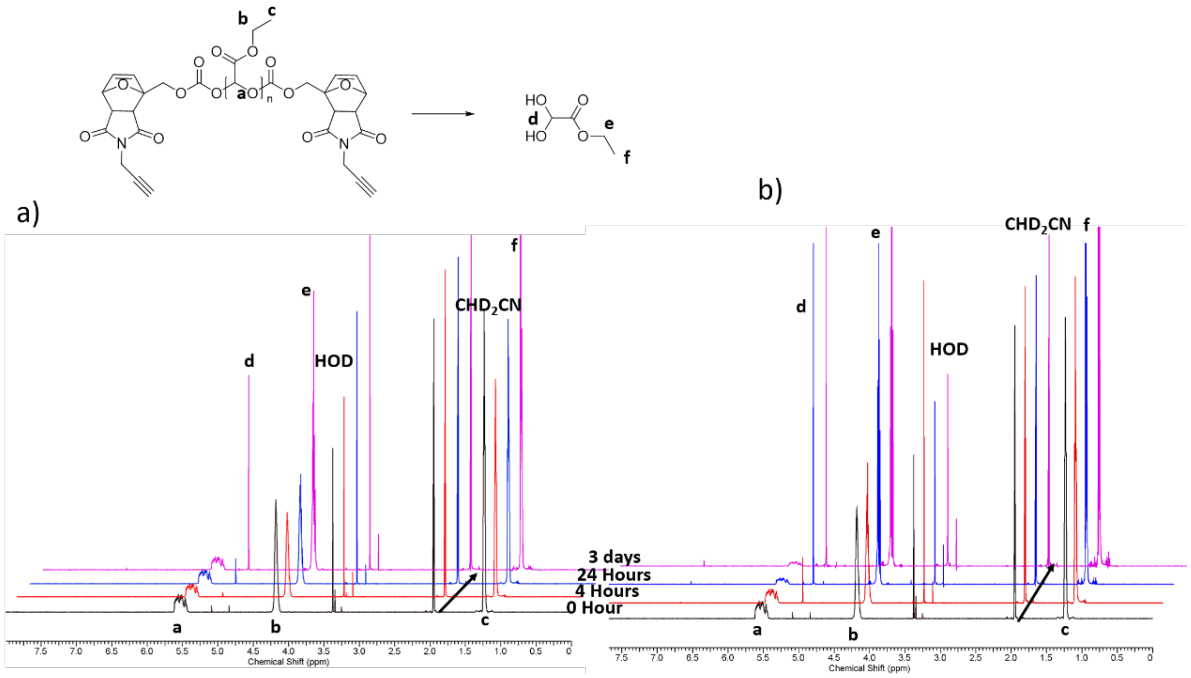

Figure S25. ^{1}H NMR spectra of **PEtG-DA-alkyne** incubated in 9:1 CD_3CN:D_2O at a) 40 °C and b) 60 °C. Spectra are offset to allow the progression over time to be clearly observed.

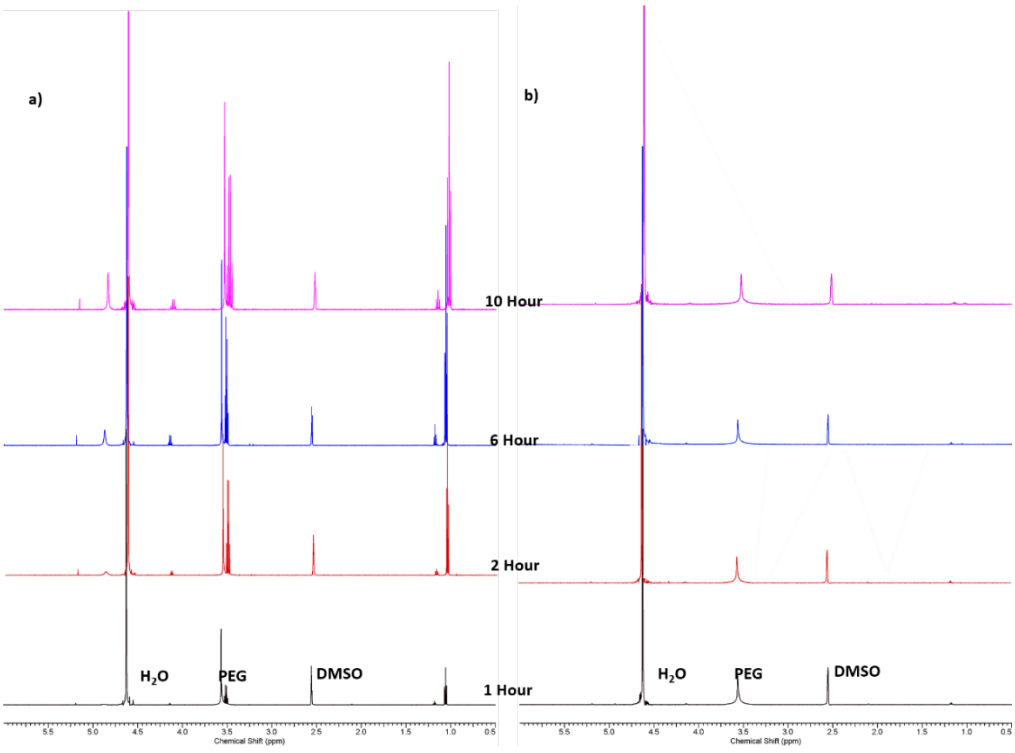

Figure S26. ^{1}H NMR spectra of **PEtG-DA-PEO5000** micelles incubated in 5:1 DMSO-d_6:D_2O at a) 75 °C and b) 22 °C.

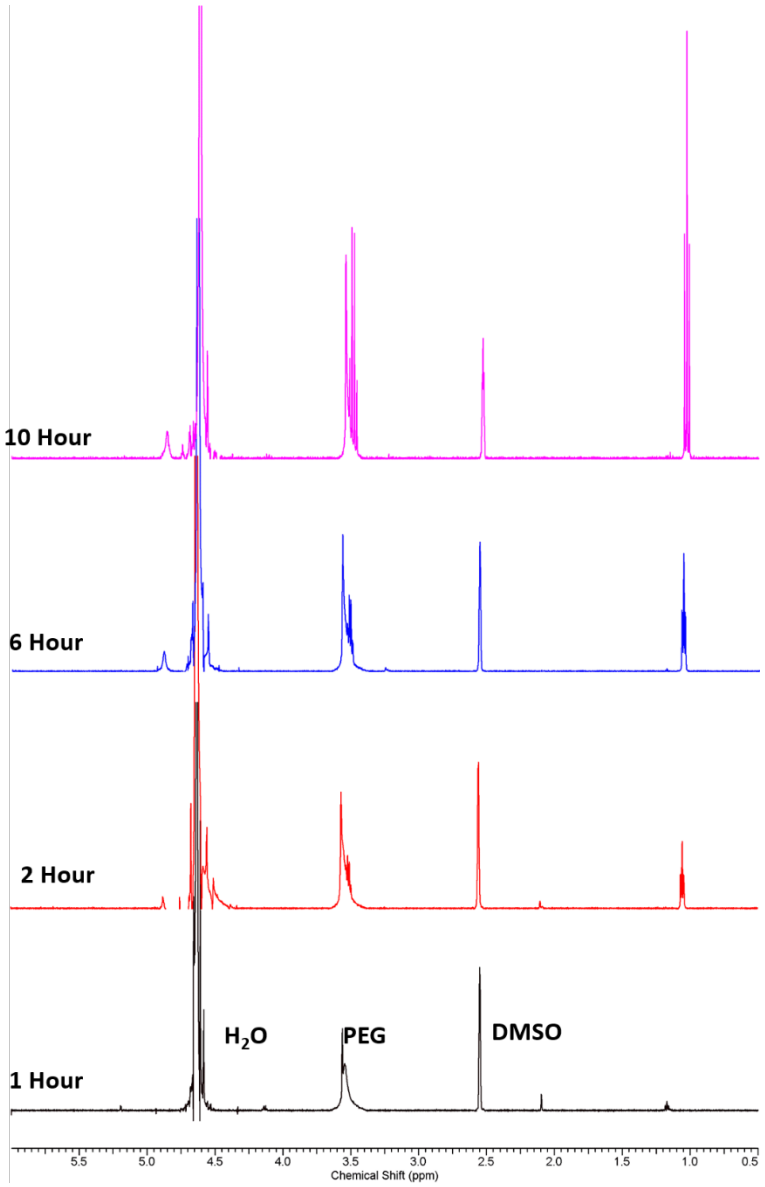

Figure S27. ^{1}H NMR spectra of **Micelle-control** incubated in 5:1 DMSO-d_6:D_2O at 75 °C.

4. TGA curves of end-caps and polymers

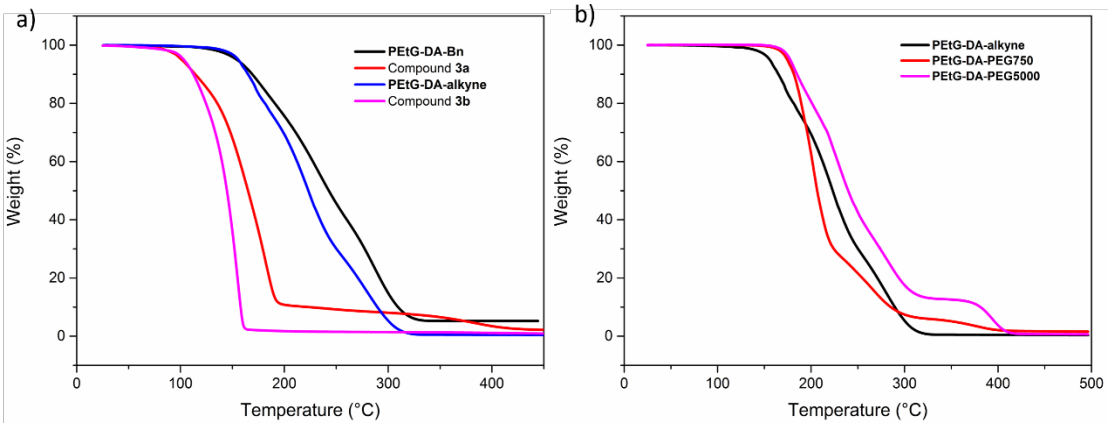

Figure S28. TGA curves of thermo-responsive a) end-caps and polymers; b) homopolymer PEtG compared with the PEtG-PEG block copolymers. It can be noted that the polymers were more thermally stable than the DA adduct itself (compound **3a** or **3b**), which degraded at ~100 °C. There are two possible explanations for this phenomenon: 1) the polymer may serve as a matrix to protect the end-cap decomposition; 2) the elimination reaction following the retro-DA reaction is the rate-limiting step for thermal depolymerization. In the block copolymers, the presence of a second decomposition step at 300 °C provides can be attributed to the PEG block.

Table S1. Molecular weights, measured by SEC in THF relative to PMMA standards, for the polymers, and thermal properties as measured by TGA. T_O = onset degradation temperature measured by TGA.

Polymer	M_n (SEC) (kg/mol)	Dispersity ($Đ$)	T_O (°C)
PEtG-DA-Bn	33	1.8	169
PEtG-control[1b]	42	1.4	N/A
PEtG-DA-alkyne	63	2.0	154
PEtG-DA-PEG750	59	1.9	177
PEtG-DA-PEG5000	35	2.0	171
Micelle-control[1a]	40	2.1	N/A
Vesicle-control	77	2.3	N/A

5. SEC traces for polymers

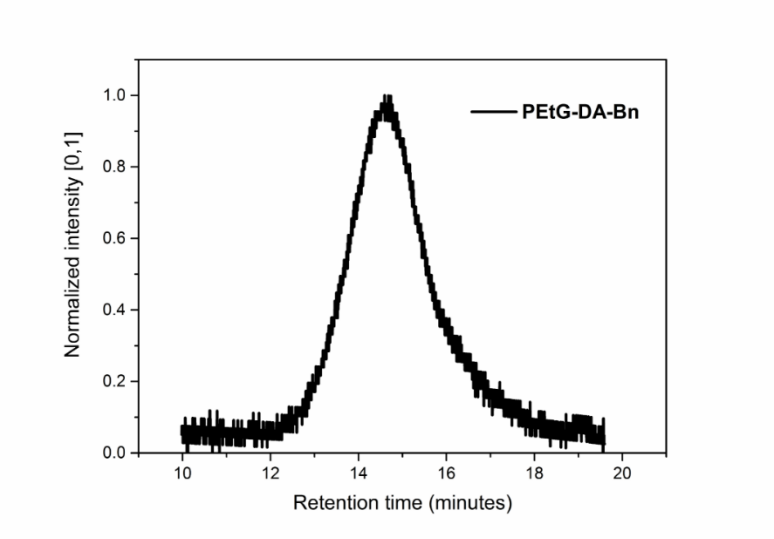

Figure S29. SEC curve of **PEtG-DA-Bn**.

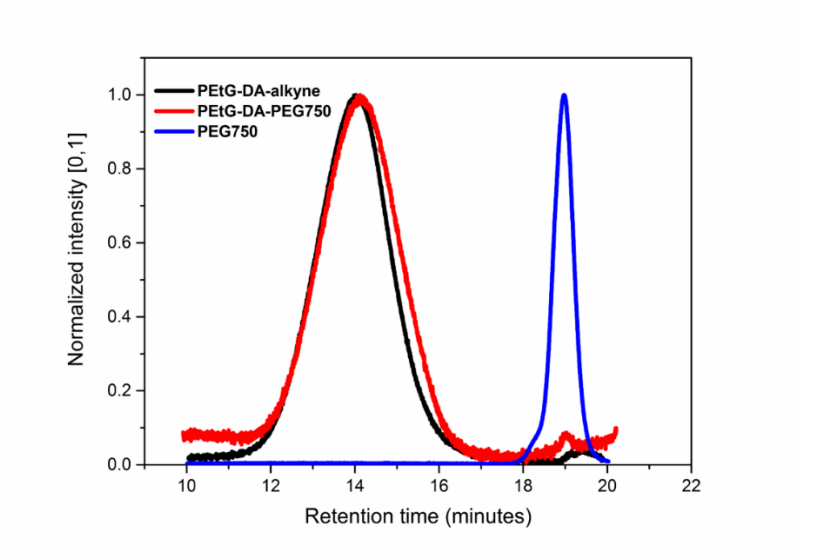

Figure S30. Comparison of SEC curves of **PEtG-DA-alkyne**, PEG 750 g/mol, and **PEtG-DA-PEG750**. No increase in molar mass was observed upon coupling of PEG, which is consistent with previous work and can be attributed to the small mass fraction of the PEG as well as possible conformational changes that would cancel the effects of the addition of mass. This is consistent with our previous reports.[1a, 6]

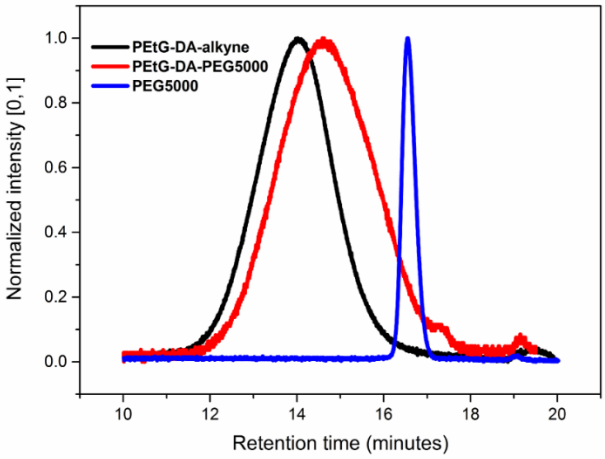

Figure S31. Comparison of SEC curves of **PEtG-DA-alkyne**, PEG 750 g/mol, and **PEtG-DA-PEG5000**. As THF is not an ideal solvent for PEG, after coupling with PEG5000, the hydrodynamic radius of **PEG-DA-PEG5000** decreased rather than increased likely due to some polymer chain collapse. However the absence of a free PEG peak combined its presence in the NMR spectra clearly confirmed the presence of PEG in the block copolymer.

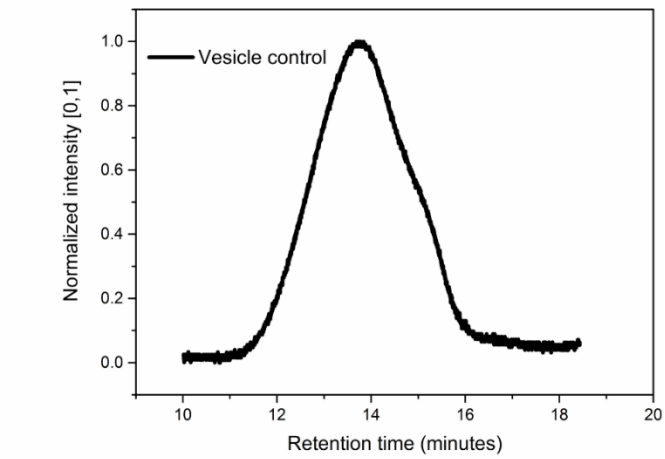

Figure S32. SEC curve of **Vesicle-control**.

6. DLS distributions of all assemblies

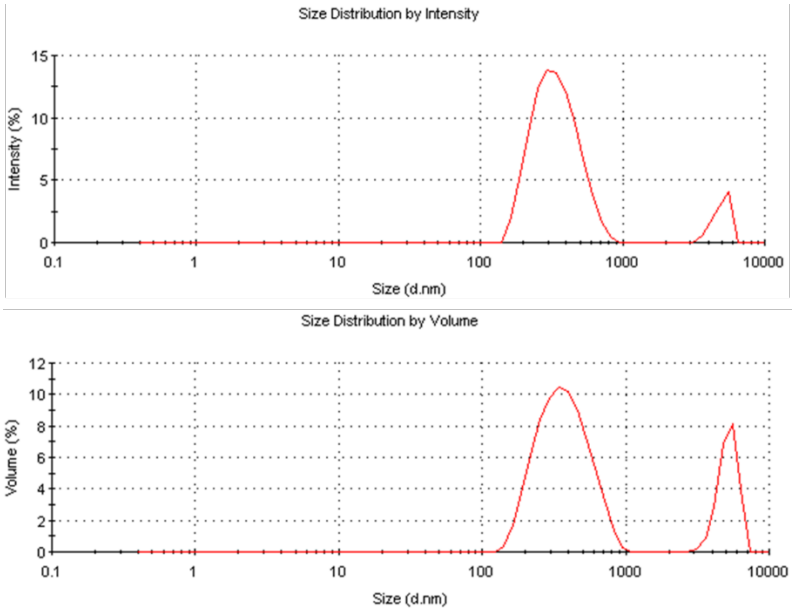

Figure S33. DLS intensity (top) and volume (bottom) distributions for **PEtG-DA-PEG750** vesicles.

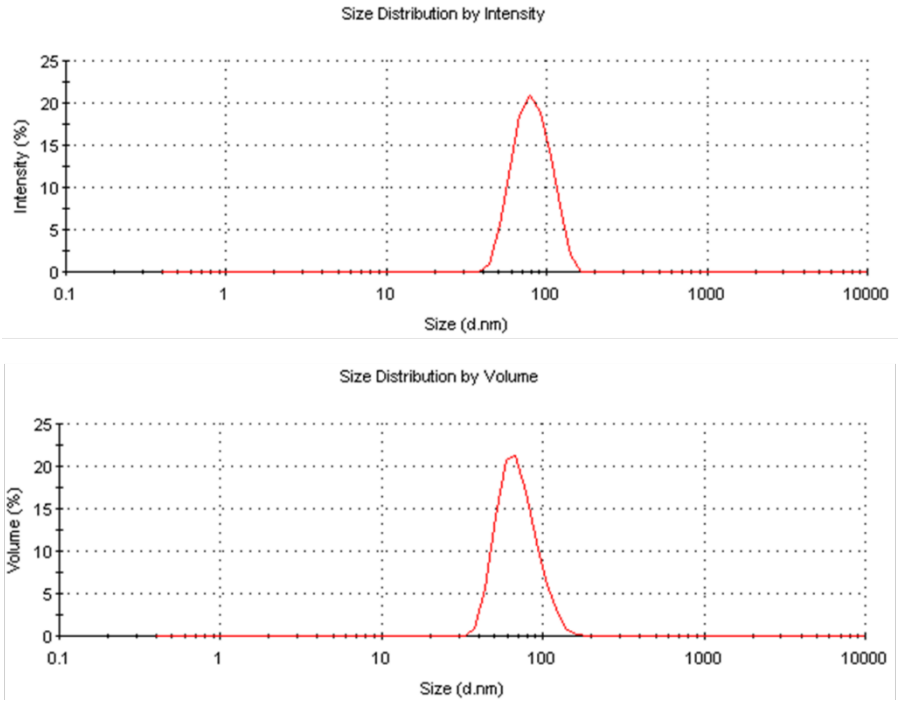

Figure S34. DLS intensity (top) and volume (bottom) distributions for **PEtG-DA-PEG5000** micelles.

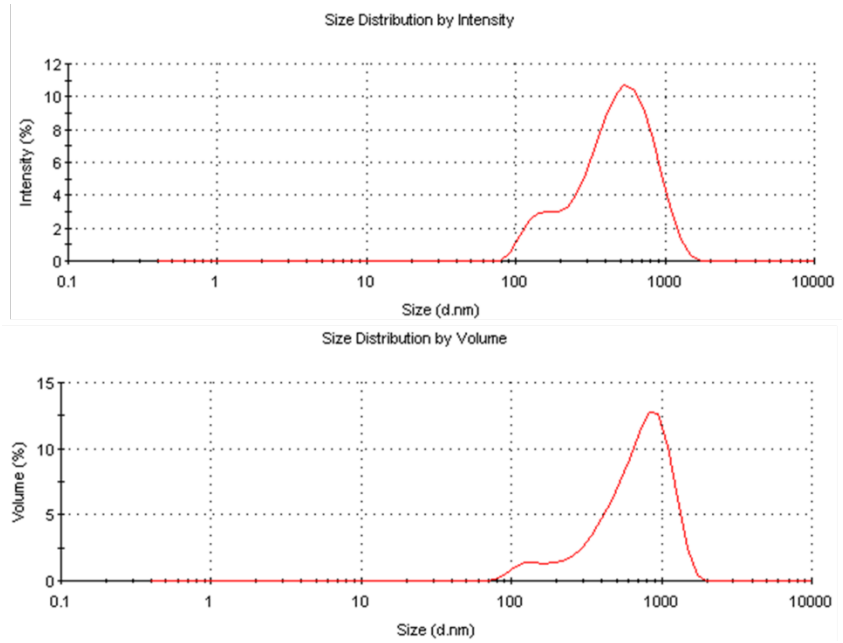

Figure S35. DLS intensity (top) and volume (bottom) distributions for **Vesicle-control**.

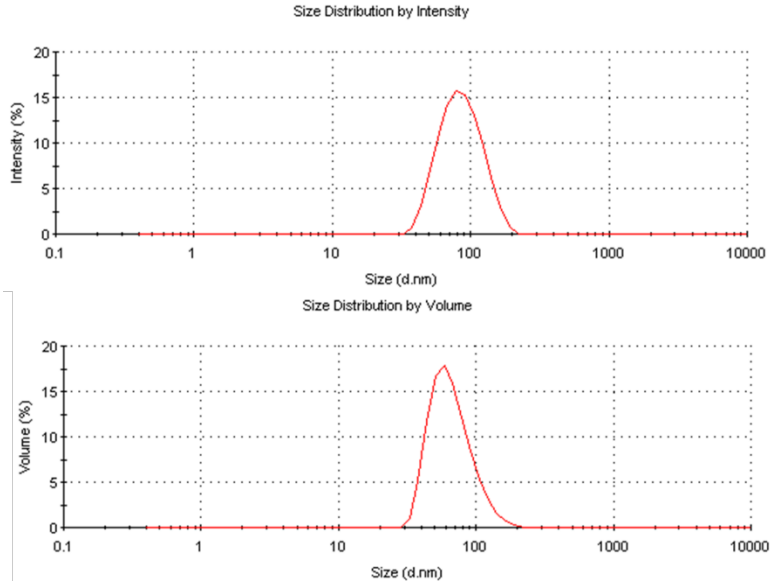

Figure S36. DLS intensity (top) and volume (bottom) distributions for **Micelle-control**.

7. Additional TEM images

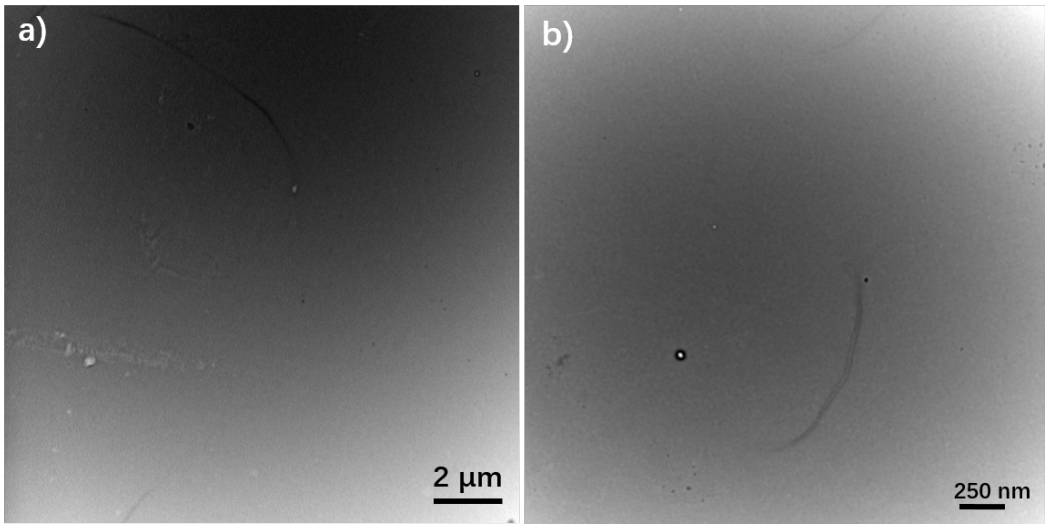

Figure S37. TEM images of a) **PEtG-DA-PEG750** vesicles and b) **PEtG-DA-PEG5000** micelles after incubation at 75 ˚C for 16 h. No assemblies were observed.

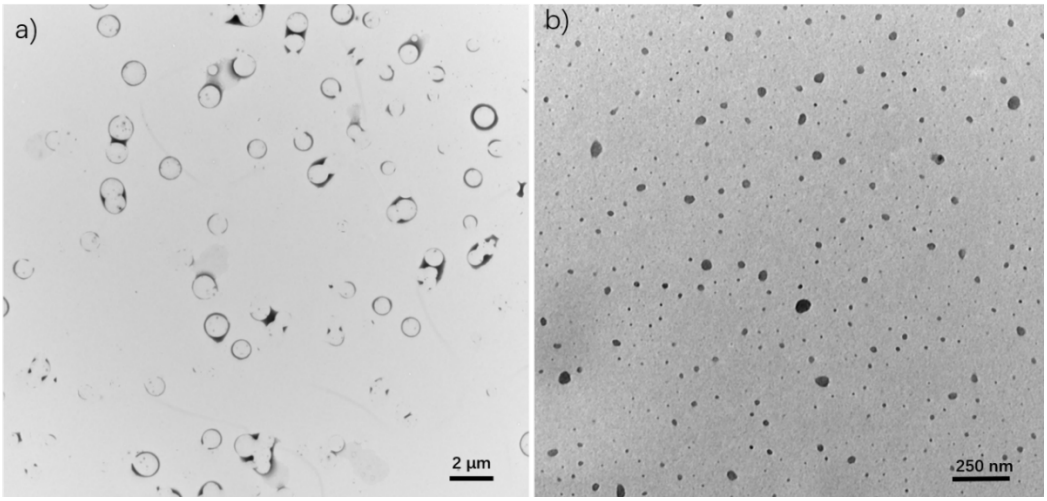

Figure S38. TEM images of a) **Vesicle-control** and b) **Micelle-control**.

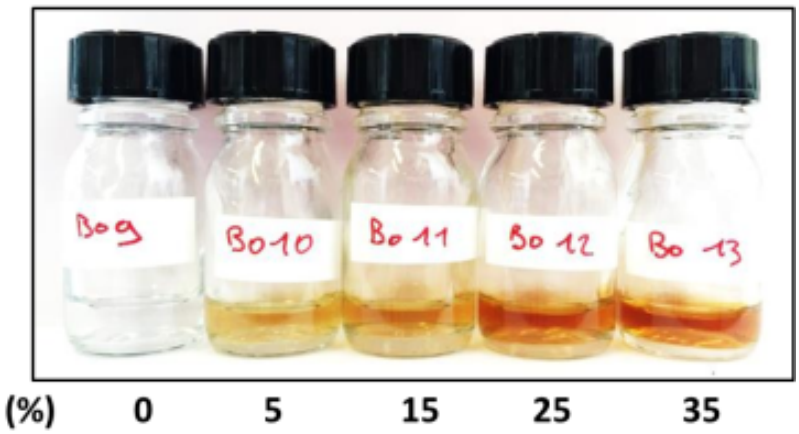

Figure S39. Photos of IONP-loaded **PEtG-DA-PEG5000** micelles with increasing mass % of IONP.

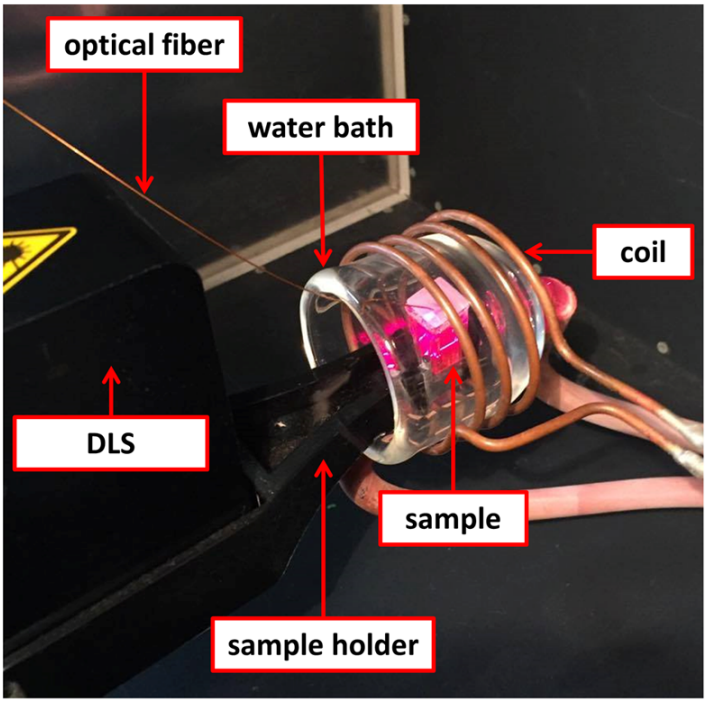

Figure S40. Photo of the dynamic light scattering magnetic hyperthermic set-up.

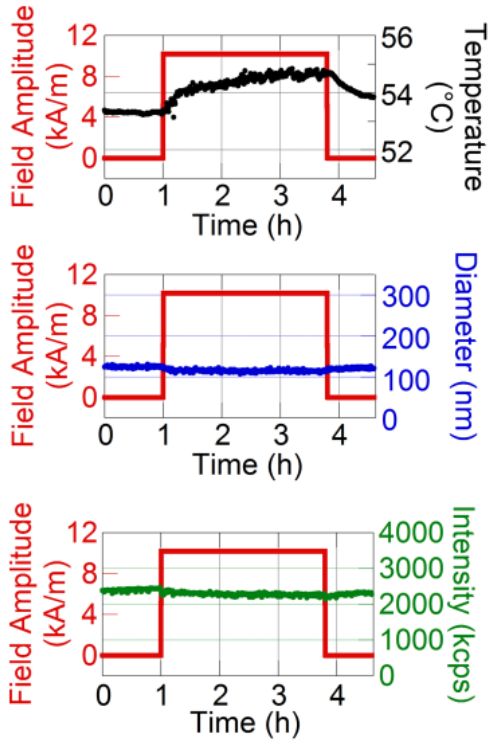

Figure S41. Bulk temperature, particle diameter, and count rate measured before, during, and after magnetic hyperthermia using an *in situ* DLS for IONP-loaded **PEtG-DA-PEG5000** with a bulk temperature of 53 °C.

8. Study of the thermal degradation by small angle neutron scattering

The thermal degradation of the thermosensitive micelles was also investigated by small-angle neutron scattering (SANS). Micelles loaded with IONPs were prepared as previously described, with few changes to adapt to this other characterization technique. The IONPs (d_{TEM}=10.5 nm) and the polymer were mixed in deuterated THF, and nano-precipitated in deuterated water to improve the contrast between the micelles and their solvent. Pure **PEtG-DA-PEG5000** micelles (BO14) or magnetically loaded thermosensitive micelles (BO15, 35 mass% iron oxide relative to polymer) were prepared this way, at a concentration of 0.6 mg·mL^{-1}. The effect of long heating on the structure of the micelles was evidenced by comparing the SANS curves (Fig. S42) before

and after heating at 80 °C in an oven for 30 min. The curves of micelles before heating were well fitted by a polydisperse sphere form factor multiplied by a "sticky hard sphere" structure factor to take into account short-range attractions. The fitted radius and volume fraction of the micelles were respectively R_0=10.9 nm and ϕ=0.00028 (R_0=11.7 nm and ϕ=0.00030) for the unloaded micelles BO14 (respectively magnetically loaded micelles BO15) with a high dispersity σ=0.4 (Log-normal distribution) in both cases. The weight-average radius of the micelles that take into account this Log-normal dispersity can be calculated using $R_w = \langle R^4 \rangle / \langle R^3 \rangle = R_0 \cdot \exp(7\sigma^2/2)$, leading to R_w=19.1 nm for pure micelles and R_w=20.5 nm for magnetic ones. These SANS sizes are still much lower than the hydrodynamic radius of the micelles found around 50 nm. However, this can be explained by the relatively high hydration level of **PEtG** blocks compared to standard hydrophobic polymers, leading to a dominant contribution to the neutron scattering contrast from the dense dehydrated cores of the micelles compared to their hydrated shells. This is also why the fitted volume fractions around 0.03 vol% are about twice lower than expected from the 0.6 mg/mL total concentration in polymer.

The curves of the heat-treated micelles were not fitted by a model shape. Nonetheless, they can be interpreted by a drastic reduction of the volume fraction of suspended copolymer micelles, together with an increase of the size of the remaining objects (as ascribed to aggregation of the remaining IONPs). This SANS experiment thus brings another evidence of the thermosensitivity of **PEtG-DA-PEG5000** copolymer micelles that did not disappear when embedding IONPs in their core.

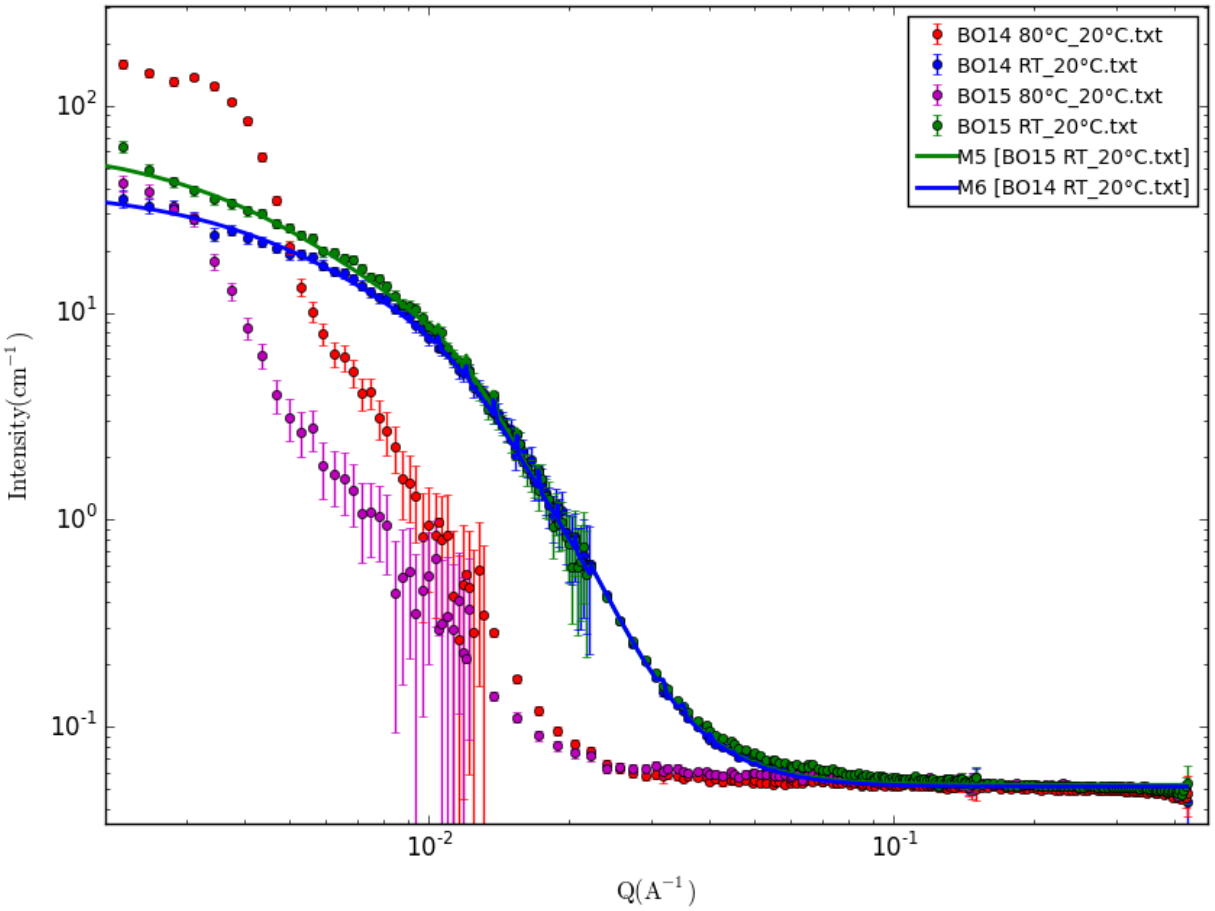

Figure S42. SANS curves of pure micelles BO14 and magnetically loaded micelles BO15 before and after treatment at 80°C for 30 min (the SANS curves being acquired afterwards, at 20°C). The curves of the untreated micelles were fitted by a polydisperse sphere form factor multiplied by a "sticky hard sphere" structure factor. Solid lines represent simulated curves using the SasView 3.1.2 software (http://sasview.org) with a polydisperse sphere form factor $P(q)$ multiplied by a "sticky hard sphere" structure factor $S(q)$ to take into account short-range attractive interactions between the micelles.[7] In addition to the SLDs that were fixed to their theoretical values, the parameters of the polydisperse sphere form factor were the volume fraction ϕ, the incoherent background level, the median radius R_0 of the micelles and the width σ of the distribution of radii as described by a Log-normal law. Other fitting parameters of the sticky hard sphere structure factor $S(q)$ were the "stickiness" τ=0.047±0.006 (respectively τ=0.036±0.0015) and the "perturbation distance" ε=0.637±0.019 (respectively ε=0.605±0.012) for the pure micelles BO14 (respectively magnetically loaded micelles BO15).

9. References

1 a) B. Fan, J. F. Trant, A. D. Wong, E. R. Gillies, *J. Am. Chem. Soc.*, 2014, ***136***, 10116-10123; b) B. Fan, J. F. Trant, R. E. Yardley, A. J. Pickering, F. Lagugné-Labarthet, E. R. Gillies, *Macromolecules*, 2016, ***49***, 7196-7203.

2 M. Sortino, V. Cechinel Filho, R. Corrêa, S. Zacchino, *Bioorg. Med. Chem.*, 2008, ***16***, 560-568.

3 M. Link, X. Li, J. Kleim, O. S. Wolfbeis, *Eur. J. of Org. Chem.*, 2010, ***2010***, 6922-6927.

4 a) G. Hemery, A. C. Keyes Jr, E. Garaio, I. Rodrigo, J. A. Garcia, F. Plazaola, E. Garanger, O. Sandre, *Inorg. Chem.* , 2017, ***56***, 8232-8243; b) D. Caruntu, G. Caruntu, Y. Chen, C. J. O'Connor, G. Goloverda, V. L. Kolesnichenko, *Chem. Mater.*, 2004, ***16***, 5527-5534.

5 G. Hemery, E. Garanger, S. Lecommandoux, A. D. Wong, E. R. Gillies, B. Pedrono, T. Bayle, D. Jacob, O. Sandre, *J. Phys. D: Appl. Phys.*, 2015, ***48***, 494001.

6 B. Fan, E. R. Gillies, *Mol. Pharmaceutics*, 2017, **14**, 2548.

7 a) R.J. Baxter, *J. Chem. Phys.* 1968, ***49***, 2770-2774; b) S. V. G. Menon, C. Manohar, K. S. Rao, *J. Chem. Phys.* 1991, ***95***, 9186-9190